Journal of Physiology (1990), **426**, *pp.* 43–80
With 19 *figures*
Printed in Great Britain

ELECTROPHYSIOLOGY OF GLUTAMATE AND SODIUM CO-TRANSPORT IN A GLIAL CELL OF THE SALAMANDER RETINA

BY E. A. SCHWARTZ AND M. TACHIBANA*

From the Department of Pharmacological and Physiological Sciences, The University of Chicago, 947 E. 58th Street, Chicago, IL 60637, USA

(*Received 18 July 1989*)

SUMMARY

1. Müller cells were isolated from salamander retinas and their membrane voltage was controlled with a whole-cell voltage clamp. External D-aspartate, L-aspartate and L-glutamate each induced a membrane current. D-Glutamate, kainate, quisqualate and *N*-methyl-D-aspartate were more than 100× less effective than L-aspartate. Kynurenic acid had no effect on the current produced by L-glutamate, L-aspartate or D-aspartate.

2. The current induced by an acidic amino acid (AAA) was completely dependent on the presence of external Na^+. Neither Li^+, Cs^+, choline nor TEA^+ were able to substitute for Na^+. The relationship between external Na^+ concentration and current amplitude can be explained if the binding of three Na^+ ions enabled transport. The apparent affinity constant for Na^+ binding was 41 mM. Altering K^+, H^+ and Cl^- concentrations demonstrated that these ions are not required for transport.

3. The shape of the current–voltage relation did not depend on the external amino acid concentration. The relationship between D-aspartate concentration and current amplitude can be described by the binding of D-aspartate to a single site with an apparent affinity constant of 20 μM.

4. Influx and efflux of AAA were not symmetric. Although influx was electrogenic, efflux did not produce a current. Moreover, influx stimulated efflux; but efflux inhibited influx.

5. Removing external Na^+ demonstrated that Na^+ carried a current in the absence of an AAA. Li^+ was a very poor substitute for Na^+. This current may be due to the uncoupled movement of Na^+ through the transporter. The relationship between the external Na^+ concentration and the amplitude of the uncoupled current can be explained if the binding of two or three Na^+ ions enabled the translocation of Na^+ in the absence of an AAA. The apparent affinity constant for Na^+ binding was approximately 90 mM.

6. The temperature dependence of the AAA-induced current had a Q_{10} between 8 and 18 °C of 1·95. The Q_{10} is consistent with a rate constant for influx of 10^4 s^{-1} (at −70 mV and 20 °C). The maximum rate of influx was measured following a concentration jump produced by the photolysis of 'caged' L-glutamate. The onset of

* Present address: Department of Psychology, The University of Tokyo, Tokyo 113, Japan.

the observed current was limited by the 1·3 ms resolution of the recording system. Hence, the rate constant for influx must be faster than 10^3 s^{-1}.

7. These results can be explained by a model in which Na^+ and an AAA bind at sites outside the membrane's voltage field and move as a multi-ion complex through a pore-like structure. The model has three binding sites for Na^+ at the external surface and only one binding site for Na^+ at the internal surface. The asymmetry in Na^+ binding produces an electrogenic influx and an electroneutral efflux. Inward and outward components of the current induced by an external AAA can be explained if co-transport and uncoupled Na^+ flux are both mediated by the same transporter.

8. Müller cells had large K^+ conductances which determined the resting potential and input resistance. Because the input resistance was low, activation of the AAA transporter produced only a few millivolts of depolarization.

9. The concentration of an AAA in the restricted extracellular space of a tissue should be a steep function of membrane voltage. Müller cells normally maintain a relatively constant hyperpolarization and continuously accumulate AAA. During pathological conditions, when Müller cells are depolarized, extracellular AAA concentration would increase.

INTRODUCTION

Carriers can remove glutamate or γ-aminobutyric acid (GABA) from a synaptic cleft and transport these amino acids into glia and selected neurons (see Bennett, Mulder & Snyder, 1974). Uptake can terminate synaptic transmission and can regulate the extracellular concentration maintained between periods of transmission. Control of the maintained glutamate concentration is particularly important. Prolonged elevation of the extracellular glutamate concentration leads to neuron death (Olney, Ho & Rhee, 1971) and may be part of the etiology of several forms of brain pathology, including ischaemic brain damage (see Choi, 1988). In addition to their uptake role, carriers may also function to release amino acids at some synapses (Schwartz, 1982; Nelson & Blaustein, 1982; Miller & Schwartz, 1983). The mechanism for release has been suggested to involve an ability of voltage to regulate electrogenic transport. Recently, electrogenic glutamate transport has been observed in a glial cell (Brew & Attwell, 1987; Barbour, Brew & Attwell, 1988). We have re-investigated the electrophysiology of glutamate transport in order to understand better how voltage controls uptake and release. We conclude by considering the functional consequences of voltage sensitivity and propose a model of the transport mechanism.

METHODS

Experiments utilized salamanders, *Ambystoma tigrinum*, that were in their aquatic phase. The procedure for dissociating the retina and maintaining solitary cells was similar to that described previously (Bader, MacLeish & Schwartz, 1978). A salamander was decapitated and pithed. The eyes were enucleated and hemisected. The posterior parts were placed in a test-tube containing 10 ml of saline with 2 mg ml^{-1} papain (Calbiochem, USA). The composition of the saline was (in mM): NaCl, 108; KCl, 1·5; $MgCl_2$, 0·5; $NaHCO_3$, 0·5; HEPES, 2; pyruvate, 1; glucose, 15; and pH 7·4. The tissue was incubated with gentle rocking for 20 min at room temperature. Retinas were

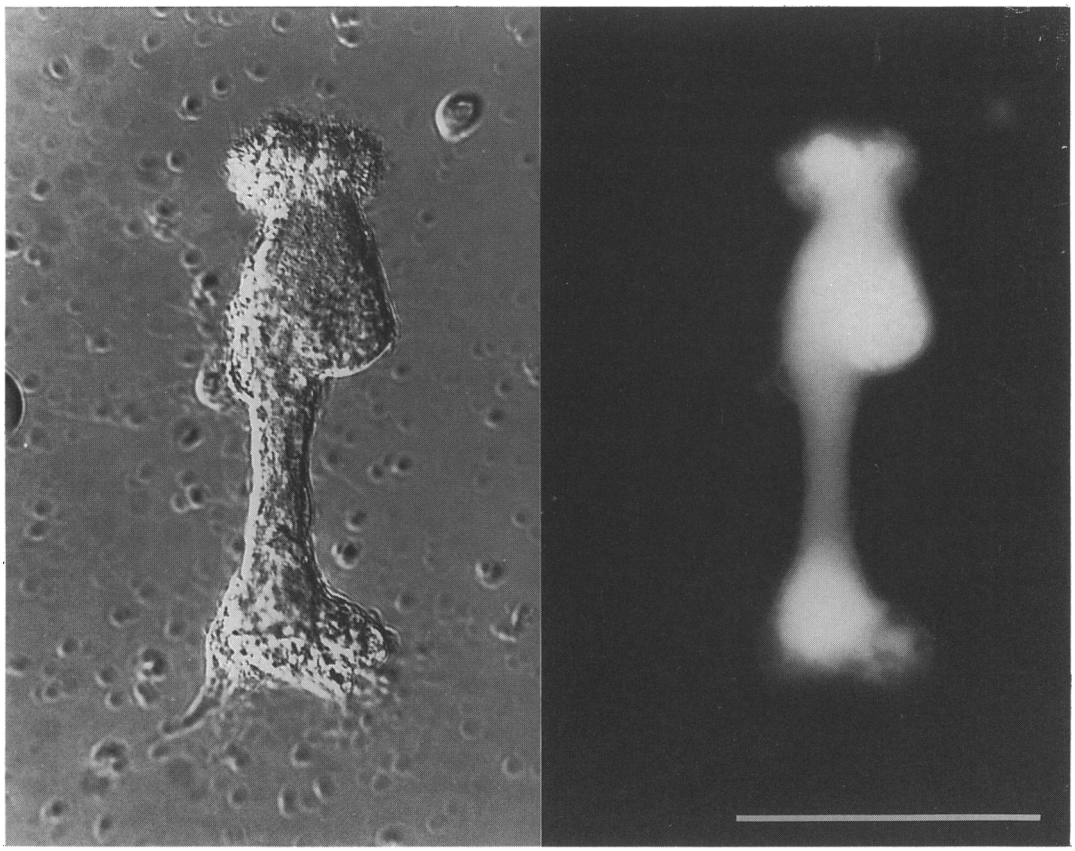

Fig. 1. A solitary Müller cell isolated from the salamander retina. The cell was incubated for 60 min in a medium containing 10 μM-BCECF/AM. The micrograph at the left was viewed with Hoffman interference optics. The micrograph at the right was viewed with fluorescence optics and shows a relatively homogeneous intracellular distribution of fluorescent BCECF superimposed on apparent staining of nuclear chromatin. After these pictures were taken, this cell was used for the experiment of Fig. 6*B*. The horizontal bar indicates 50 μm.

then separated from the pigment epithelium and incubated in a fresh enzyme solution for an additional 25 min. The retinas were rinsed in saline containing an added 1 mg ml^{-1} bovine serum albumin and then triturated with a large tip (approximately 1·5 mm internal diameter) pipette. A few drops of the resulting cell suspension were placed in a shallow dish whose bottom was a cover-slip modified by the covalent attachment of concanavalin A (DeVries & Schwartz, 1989). After approximately half an hour, cells adhered to the cover-slip and 3 ml of saline (see above) with 2 mM-Ca^{2+} and 0·1 mg ml^{-1} bovine serum albumin were added. Dishes were kept at 15 °C prior to being used in electrophysiological experiments. Retinal glial cells, Müller cells, were identified by their characteristic morphology (Fig. 1, left panel).

A dish containing cells was mounted on the stage of an inverted microscope. A stainless-steel ring was inserted into the dish to reduce the volume of liquid required to fill the central part of the dish. Solutions were pumped to the dish at 0·5 ml/min through a Teflon tube (0·8 mm internal diameter) and removed by suction. The procedures for making pipettes from borosilicate glass, sealing a pipette to the surface of a cell, and recording membrane current were similar to those described by Hamill, Marty, Neher, Sakmann & Sigworth (1981) for a 'whole-cell, tight-seal' voltage clamp. The

resistance of a fire-polished pipette was approximately 3 MΩ. Series resistance during a whole-cell recording was approximately 15–30 MΩ. Consequently, a 100 pA current produced an error of less than 3 mV. Usually no correction was made; exceptions are noted in the figure legends. Pipette capacitance was electronically cancelled. The experiments illustrated in Fig. 16 required a high-frequency response. In this case, the tip diameter was increased slightly so that series resistance was approximately 10 MΩ and the pipettes were coated with Sylgard to decrease their capacitance.

Voltage-dependent K^+ and Ca^{2+} currents (Newman, 1985*a*) as well as a voltage-dependent Na^+ current (unpublished observation) can be observed in Müller cells. K^+ currents were reduced by replacing K^+ in the internal and external media with Cs^+ (or TEA^+); Ca^{2+} currents were reduced by omitting Ca^{2+} from the external medium; Na^+ currents were blocked with TTX. The external saline contained (in mM): NaCl, 98; CsCl, 10; $MgCl_2$, 3·5; HEPES, 2; D-glucose, 15; TTX, 1 μM; and pH 7·4. In most experiments, the patch pipette contained (in mM): CsCl, 70; NaCl, 20; Cs_2EGTA, 10; $CaCl_2$, 1; HEPES, 2; and pH 7·0. Exceptions are noted in the figure legends. After K^+, Ca^{2+} and Na^+ currents were blocked the cell resistance was $3{\cdot}35 \pm 1{\cdot}37$ GΩ (mean ± S.D. for a series of sixty-two cells) and the capacitance was 150 ± 64 pF (see text associated with Fig. 7). When these currents were not blocked the apparent input resistance at the resting potential was approximately 30 MΩ (see text associated with Fig. 17).

The solution surrounding a cell could be changed by directing a stream of fluid at the cell from a nearby 'puffer' pipette. In some experiments multiple puffer pipettes were used. Three puffer pipettes could be fabricated from a single piece of triple-barelled glass and held by one micromanipulator. In addition, D-aspartate or L-glutamate could be ionophoresed from a micropipette (100–200 MΩ) containing 0·1 M-caesium D-aspartate or caesium L-glutamate (pH 8·0) that was positioned a few micrometres from the cell surface. The amino acid was ejected by pulses of −4 to −15 nA for between 0·1 and 10 s. The leakage of amino acid between pulses was reduced by a current of 0·5–2 nA.

The solution in the patch pipette could be changed several times during the course of an experiment (Figs 5*A*, 10, 13*B* and 17). Three tubes were introduced into the back of the patch pipette and brought within 100 μm of the tip (for a similar but not identical method, see Soejima & Noma, 1984). Two of these tubes were inlets and one tube was an outlet. Each tube was connected to a 1 ml syringe whose plunger position was controlled by a motor-driven micrometer. The motion of each micrometer could be separately controlled. It was important to balance the inlet and outlet rates in order to prevent a change in cell volume. An increase in cell volume produced an irreversible increase in an outwardly rectifying leak current. One inlet tube contained the same solution as the patch pipette. The second inlet contained a test solution. The experiment began with the control solution flowing from the first inlet. Stopping the micrometer drive attached to the first inlet and turning on the micrometer drive attached to the second inlet changed the internal solution within the cell in less than 2 min. The procedure could be reversed and repeated several times. Control experiments demonstrated that an outward K^+ current was blocked during internal perfusion with a K^+-poor solution and was restored after returning to a K^+-rich solution (see Fig. 5).

The dependence of current on membrane voltage was often measured while the voltage was 'ramped' over an extended range. Accuracy was increased by averaging six to twelve traces while a cell was bathed in saline and then averaging a similar number of traces during exposure to an AAA. The difference was the AAA-induced current. It was often possible to repeat the entire procedure two to ten times and verify that all of the averaged responses were similar. The averaged currents are displayed in the figures.

The release of L-glutamate was detected with an assay that utilized the enzyme glutamate dehydrogenase and measured the production of NADPH (Korenbrot, Perry & Copenhagen, 1987; Nicholls, Sihra & Sanchez-Prieto, 1987). The enzyme (Boehringer Mannheim Gmbh, FRG) was dialysed against a solution containing (in mM): NaCl, 98; CsCl, 10; $MgCl_2$, 3·5; and 2 mM-phosphate buffer pH 7·4 and diluted to a final concentration of 1 mg ml^{-1}. Both NADP and ADP, which increase the efficiency of the enzyme, were added to a final concentration of 2 mM. Cells were plated into a dish whose bottom was a glass cover-slip treated with poly-lysine (a cover-slip derivatized with a silane, glutaraldehyde and concanavalin A produced a faint fluorescence and, consequently, could not be used). The external medium was the enzyme solution. To facilitate the detection of small quantities of NADPH, the extracellular volume was reduced by adapting the method of Kuffler & Yoshikami (1975) as follows. A pipette containing the external medium was connected

to the electrical ground of the recording system and positioned with its tip immediately adjacent to a cell. Next, a patch pipette was sealed to a cell. Then, approximately 150 μl of perfluorinated oil (Fluorinert-40, 3M, USA) was introduced into the dish. Although the oil is denser than water, surface tension maintained the oil above the aqueous phase. The volume of the aqueous phase was slowly reduced until only a shallow layer of external saline remained beneath the oil. An ionophoretic pipette containing D-aspartate was positioned in the oil above the cell. At the appropriate moment during an experiment, the ionophoretic pipette could be lowered into the aqueous phase. The light from a 75 W xenon lamp was collected by quartz optics, filtered to pass 360 nm (two 10 nm half-bandwidth, six-cavity filters were placed in series), and focused onto a single cell by a Zeiss neofluor 100 × /1·3 NA objective. An immersion oil was selected for low fluorescence (type FF, Cargille, USA). Fluorescent light between 470 and 570 nm was passed by an interference filter and measured with a photomultiplier tube (type 9924B, Thorn-EMI, UK) operated for photon counting. Fluorescent light and membrane current were recorded during 30 s voltage steps.

Internal pH was measured with the fluorescent dye BCECF (Rink, Tsien & Pozzan, 1982). Cells were incubated for 60 min in media containing 10 μM of the acetoxymethylester BCECF/AM and then superfused with media lacking the dye. BCECF is trapped within a cell (Fig. 1, right panel) after endogenous esterases cleave acetoxymethylester groups. Epi-illumination was restricted to a single cell by a diaphragm placed in a back focal plane of the microscope objective. A stepping motor alternately inserted 440 and 500 nm (10 nm half-bandwidth) filters into the light path. Each filter was inserted for a 1 s interval and the fluorescent light emitted from the cell at 530 nm (40 nm half-bandwidth) was measured with a photomultiplier tube. Fluorescence during illumination with 500 nm light was sensitive to pH; fluorescence during illumination with 440 nm light was relatively insensitive to pH. The ratio of the fluorescence measured at the two illuminating wavelengths compensated for small changes in dye concentration and cell shape that might occur during an experiment. A calibration curve for the conversion of fluorescence ratio to pH was determined from single cells that were permeabilized to protons with the carrier nigericin (10 μM) and then superfused with solutions that were buffered with 10 mM-HEPES and 10 mM-MES to a series of pH values between 5·6 and 8·8. Cells that had not been incubated in BCECF/AM had no detectable fluorescence.

Internal K^+ concentration was measured with the dye PBFI (Molecular Probes, USA). Illumination was restricted to a region that excluded the patch pipette. The wavelength of the incident light was alternately 360 or 400 nm (10 nm half-bandwidths). Fluorescence was measured at wavelengths longer than 455 nm. Extraneous light came from two sources: (i) autofluorescence from the cell and (ii) fluorescence excited by scattered light that reached dye in the patch pipette. Measurements were corrected for both sources of extraneous light. Autofluorescence from the cell was measured at the beginning of each experiment before a patch pipette was positioned in the field of view. Fluorescence from the patch pipette was measured at the end of each experiment after the cell was moved out of the field of view. A calibration curve for the conversion of fluorescence ratio to K^+ concentration was determined from single cells that were permeabilized to K^+ and Na^+ with the carriers valinomycin (10 μM), monensin (10 μM) and nystatin (10 μM), and then superfused with a series of Na^+-free solutions containing K^+ and choline mixtures.

Sodium microelectrodes were fabricated from micropipettes exposed to trichloromethylsilane and dried at 150 °C. The tips were filled by suction over a distance of approximately 200–300 μm with the Na^+-sensitive neutral resin ETH 227 (Steiner, Oehme, Ammann & Simon, 1979). Each pipette was individually calibrated and produced a 57 mV response for a 10-fold change in Na^+ concentration.

A 'caged' glutamate analogue, *N*-(3,4-dimethoxy-6-nitrobenzyl)-L-glutamate, was synthesized by Molecular Probes (USA). The dimethoxybenzyl group has been used previously to generate inactive compounds that can be photolysed by 320–370 nm light to release an active molecule (see Lester & Nerbonne, 1982). Caged glutamate was delivered to a cell from a puffer pipette and photolysed by a flash from a xenon flash lamp (Chadwick-Helmuth Co., USA). The light was projected unfiltered into the back focal plane of the microscope objective and filled the entire field of view. The lamp produced a flash that decayed with a time constant of approximately 150 μs. The time constant for the photo-initiated break-down of a dimethoxybenzyl compound with a similar C–N bond is approximately 50 μs (Fidler, Ellis-Davis, Kaplan & McCray, 1988).

Abbreviations. AAA, acidic amino acid; ADP, adenosine 5′-diphosphate; BCECF, bis-carboxy

ethylcarboxyfluorescein; BCECF/AM, acetomethoxy BCECF; EGTA, ethyleneglycol-*O*,*O*′-bis-(2-aminoethyl)-*N*,*N*,*N*′,*N*′-tetraacetic acid; GABA, γ-aminobutyric acid; GDH, glutamate dehydrogenase; HEPES, 4-(2-hydroxyethyl)piperazine-1-ethanesulphonic acid; MES, 2-(*N*-morpholino)-ethanesulphonic acid; NADP, β-nicotine adenine dinucleotide phosphate; NADPH, reduced NADP; NMDA, *N*-methyl-D-aspartate; TEA^+, tetraethylammonium; TTX, tetrodotoxin.

RESULTS

Identification of a transporter current

The behaviour of AAA carriers has been extensively studied by observing the flux of radiolabelled substrates into synaptosomes and cultured cells (see Erecinska, 1987). These studies have produced a distinctive profile for the substrate selectivity, pharmacology and Na^+ dependence of AAA carriers which may be used to identify a carrier-mediated current (Brew & Attwell, 1987).

AAA carriers transport L-aspartate and L-glutamate, as well as D-aspartate, but not D-glutamate (Gazzola, Dall'Asta, Bussolati, Makowska & Christensen, 1981). A current with the same substrate selectivity is shown in Fig. 2*A*. The membrane potential of a glial cell was maintained at −76 mV by a whole-cell voltage clamp. Four puffer pipettes were positioned approximately 20 μm from the cell. Each pipette contained an amino acid solution to be tested. A 4 s puff of 20 μM-L-aspartate (trace 4 in Fig. 2*A*) or L-glutamate (trace 3) produced an inward current that exceeded 50 pA. A puff of 20 μM-D-aspartate produced a current of approximately 30 pA (trace 2). A tenfold greater concentration of D-glutamate produced a current that was less than 5 pA (trace 1). The comparison indicates that D-glutamate is 100 × less effective than either L-glutamate or L-aspartate. In contrast, D-aspartate is only approximately 2 × less effective than the L-isomers (compare traces 2 and 4).

Pharmacological agents may also help to distinguish a glutamate transporter from a glutamate-gated pore. The pharmacology of glutamate-gated pores has been intensively studied. Kainate, quisqualate and NMDA are competitive agonists often used to distinguish individual subtypes (see Foster & Fagg, 1984; Watkins & Olverman, 1987). All three agents were relatively ineffective at producing a current during the conditions of our experiments. Responses elicited by these three agents and L-aspartate are compared in Fig. 2*B*. NMDA, kainate and quisqualate were at least 100 × less effective than L-aspartate in producing a current. Similar results were obtained with three cells. An additional pharmacological test used kynurenic acid, a potent competitive antagonist at a variety of glutamate-activated pores. Kynurenic acid (1 mM) did not affect the current induced by L-glutamate (two cells), by D-aspartate (two cells) or by L-aspartate (one cell).

The small responses produced by kainate and quisqualate may not be due to activation of the carrier but instead may be due to activation of a low density of glutamate-activated pores which have been reported to occur in some glial cells (see Usowicz, Gallo & Cull-Candy, 1989). In this case, kainate and quisqualate would be even less effective for activating the transporter than estimated from Fig. 2*B*. On the other hand, the failure of NMDA to produce a response does not mean that Müller cells lack NMDA-activated pores. This subtype is blocked by extracellular Mg^{2+} (Nowak, Bregestovski, Ascher, Herbert & Prochiantz, 1984; Mayer, Westbrook & Guthrie, 1984) and would not be activated during the conditions of our experiments (−70 mV and 3·5 mM-Mg^{2+}). We have not investigated whether a low density of glutamate-activated pores occurs in Müller cells.

Carriers are also selective for the cation they co-transport. Na^+ is the only

monovalent cation that enables transport; and, in particular, Li^+ will not substitute for Na^+ (Peterson & Raghupathy, 1974). In contrast, Na^+-selective pores, like the voltage-sensitive Na^+ pore in axons (Chandler & Meeves, 1965; Hille, 1972), and the relatively non-selective cation pore activated by acetylcholine at the neuromuscular junction (Gage & van Helden, 1979), are approximately equally permeable to Li^+ and Na^+. The experiment in Fig. 2*C* shows that Li^+ only poorly substituted for Na^+. An ionophoretic pulse of D-aspartate produced an inward current when a cell was bathed in a medium containing Na^+ (trace 1). Replacing Na^+ with Li^+ reduced the steady current (indicated by the upward shift of trace 2) and greatly reduced the aspartate-induced current. Finally, when Na^+ was reintroduced into the bath, the change in steady current was reversed and a response to D-aspartate reappeared (trace 3). A similar result was obtained in three additional experiments with Li^+ and in four experiments in which Na^+ was replaced with Cs^+. Thus, Na^+ is required and neither Li^+ nor Cs^+ can substitute. Consequently, the current illustrated in Fig. 2 has, as reported by Brew & Attwell (1987), the substrate specificity, pharmacology and Na^+ dependence expected for the AAA co-transport carrier.

Which ions move?

A central problem is to identify the ions that translocate across the membrane. Certainly Na^+ and an AAA are translocated. How many ions of each type interact with the transporter? Do other ions participate? *A priori*, the most likely additional ions are K^+, H^+ and Cl^-.

External D-aspartate

To characterize the concentration dependence of the AAA-induced current, six puffer pipettes, each with a different concentration of D-aspartate, were positioned near a cell. Membrane voltage was maintained at -70 mV. A puff of each solution produced an inward current (Fig. 3*A*). The amplitude of the current is plotted as a function of D-aspartate concentration in Fig. 3*B*. The data can be fitted with a Michaelis equation

$$I = I_{max}[Asp]_o/([Asp]_o + K_{D\text{-}Asp}), \quad (1)$$

where I_{max} is the maximum current amplitude, $[Asp]_o$ is the external D-aspartate concentration, and $K_{D\text{-}Asp}$ is an apparent affinity constant. In six cells $K_{D\text{-}Asp}$ was 19 ± 2 μM (mean $\pm$ S.D.). A simple explanation that is compatible with eqn (1) would have D-aspartate interact with one binding site per transporter.

External Na^+

The carrier transports Na^+ along with an AAA. The dependence on external Na^+ concentration was observed in experiments in which the external Na^+ concentration was slowly changed. A cell was continuously superfused; an ionophoretic pipette containing caesium D-aspartate and a Na^+-sensitive microelectrode were positioned nearby. Ionophoretic pulses of D-aspartate were adjusted to produce a half-maximum response and delivered at 24 s intervals. The external saline was changed to a solution in which choline replaced 90% of the Na^+. The concentration of Na^+ in the external medium was continuously measured with the Na^+-sensitive electrode.

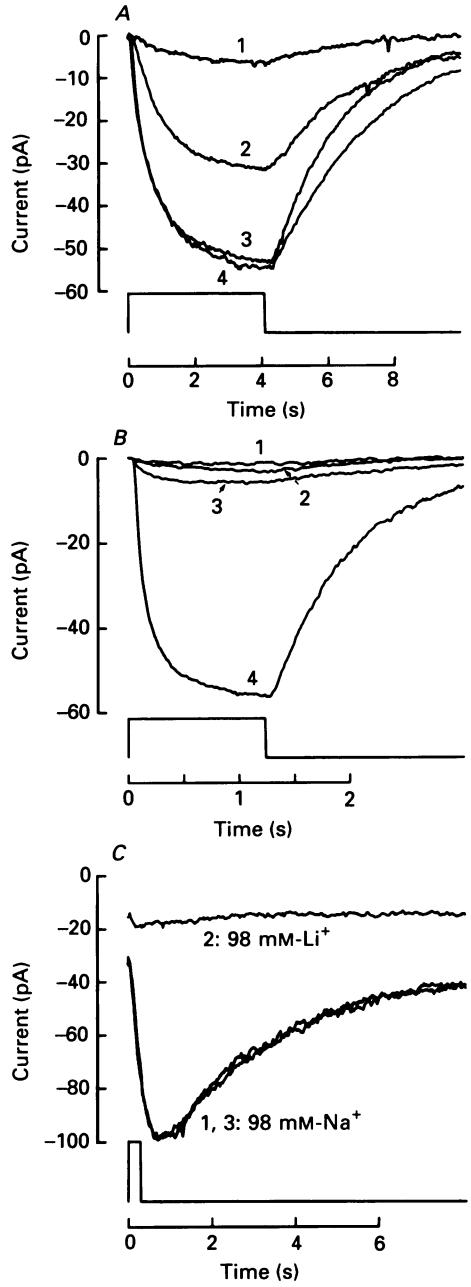

Fig. 2. Substrate specificity, pharmacology and Na^+ dependence for the AAA-induced current. *A*, substrate specificity. Four puffer pipettes were positioned near a cell. Each contained the external solution with an added amino acid. Superimposed are the currents produced by puffs of solution containing (1) 200 μM-D-glutamate, (2) 20 μM-D-aspartate, (3) 20 μM-L-glutamate and (4) 20 μM-L-aspartate. The duration of amino acid application

As the Na^+ concentration surrounding the cell was reduced, two changes were observed (Fig. 4*A*). First, the steady inward current observed in the absence of an AAA was decreased by approximately 20 pA. This change, observed in Fig. 4*A* as an upward shift in the holding current, will be considered below (Figs 12 and 14, and associated text). Second, the AAA-induced current produced by an ionophoretic pulse of D-aspartate was reduced to approximately 10% of the original amplitude. When the original Na^+-rich solution was returned to the bath, the changes were reversed. A similar sequence was observed when the same cell was first superfused with a Na^+-rich solution and then a solution in which TEA^+ replaced 90% of the Na^+. The collected data for replacing Na^+ with either choline or TEA^+ are shown in Fig. 4*B*.

The relation between the Na^+ concentration and the amplitude of the AAA-induced current is plotted in Fig. 4*B*. The AAA-induced current increased steeply as the Na^+ concentration rose above 20 mM and saturated when the concentration was greater than 70 mM. The relation between Na^+ concentration and the amplitude of the AAA-induced current can be described with the equation

$$I = I_{max}[Na^+]_o^n/([Na^+]_o^n + K_{Na}^n), \quad (2)$$

where $[Na^+]_o$ is the external sodium concentration, and K_{Na} and n are constants. The best fit for the data in Fig. 4*B* was with $n = 3$ and $K_{Na} = 43{\cdot}5$ mM. Similar results were obtained from two additional cells. The value $n = 3$ would occur if an AAA binds along with three Na^+ ions. The production of an inward current requires that at least two Na^+ ions translocate with each (negatively charged) AAA ion. Although the binding of three Na^+ ions enables transport, it is not necessary for all three Na^+ ions to pass through the membrane. For example, the binding of three Na^+ ions may enable an electrogenic influx in which two Na^+ ions leave their external binding sites and move across the membrane with one AAA molecule.

Internal potassium

An AAA transporter has been isolated from the rat brain and reconstituted into protoliposomes (Kanner & Sharon, 1978). The liposomes were reported to require internal K^+ for AAA influx. Similarly, Barbour *et al.* (1988) have reported that intracellular K^+ is essential for an AAA to produce a current in Müller cells isolated

---

is indicated by the timing trace. Membrane potential was maintained at −76 mV. *B*, pharmacological agents that operate at glutamate-activated channels are relatively ineffective in producing a current. Four puffer pipettes were positioned near a cell. Each contained a different pharmacological agent added to the external medium. Superimposed are currents produced by puffs of solution containing (1) 200 μM-*N*-methyl-D-aspartate (NMDA), (2) 200 μM-kainate, (3) 200 μM-quisqualate, and (4) 20 μM-L-aspartate. Membrane potential was maintained at −70 mV. *C*, Li^+ poorly substituted for Na^+. Superimposed are three records of total membrane current. A cell was superfused with the standard saline (containing 98 mM-Na^+). A pulse of D-aspartate, ionophoretically ejected from a nearby micropipette, produced an inward current (trace 1). The external medium was changed to a solution in which Li^+ replaced Na^+. A second ionophoretic pulse of D-aspartate produced a much smaller response (trace 2). The cell was again superfused with the Na^+-rich medium. A final pulse of D-aspartate produced a full-sized response (trace 3). Membrane potential was maintained at −70 mV.

from salamander retinas. K^+ was reported to interact at a site with an apparent affinity of 15 mM. In our experiments, we omitted K^+ from the external and patch-pipette solutions. Internal K^+ was replaced with either Cs^+, TEA^+ or choline. During the initial several minutes, the pipette solution exchanged with the cytoplasm and K^+ currents disappeared. None the less, an AAA continued to produce an

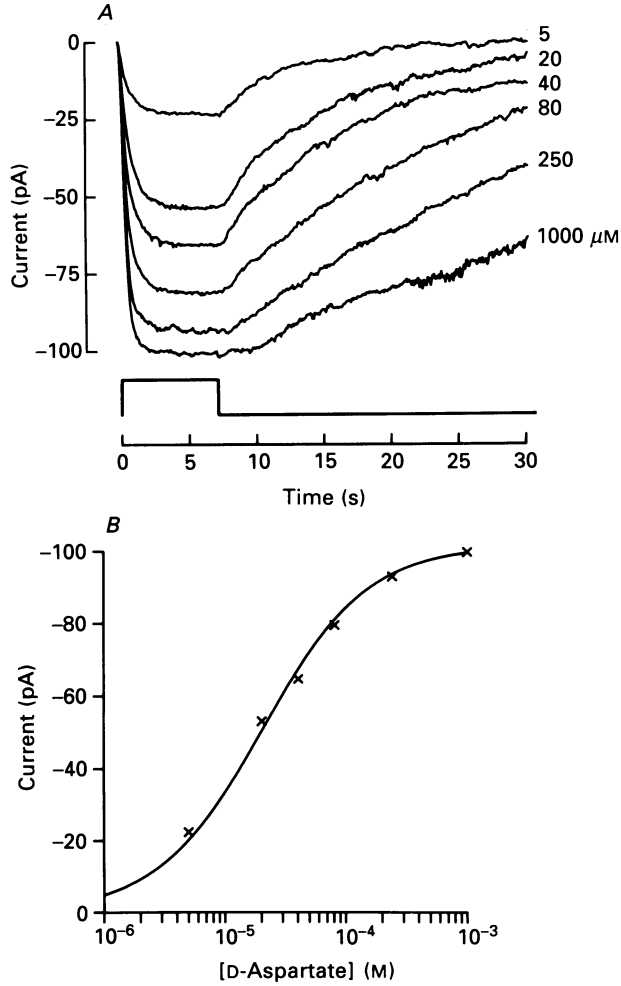

Fig. 3. Current amplitude as a function of D-aspartate concentration. Six puffer pipettes were arrayed near a cell, each containing a different concentration of D-aspartate. *A*, superimposed are currents observed during the application of 5, 20, 40, 80, 250 and 1000 μM-D-aspartate. *B*, current amplitude is plotted as a function of D-aspartate concentration. The curve is the result predicted by eqn (1) with $K_{D\text{-}Asp} = 19\ \mu M$ and $I_{max} = 101$ pA. Membrane voltage was maintained at −70 mV.

undiminished current during the entire course of an experiment that could last for an hour or more. Internal K^+ appeared not to be required. This conclusion is reinforced by the following experiment.

The patch pipette was continuously perfused with solutions that contained the K^+-sensitive fluorescent dye PBFI. Membrane current and the ratio of the fluorescence

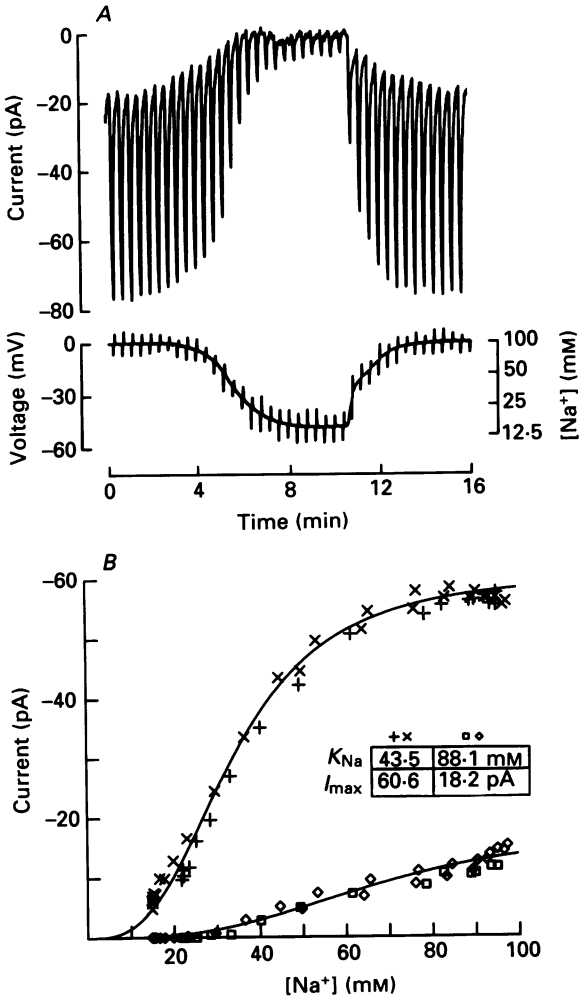

Fig. 4. The relationship between current amplitude and external Na^+ concentration. Ionophoretic pulses of D-aspartate were adjusted to produce half-maximum responses and delivered at 24 s intervals (viewing the record on an expanded time scale demonstrates that each response completely recovered before the onset of the following pulse). Extracellular Na^+ concentration was measured with a Na^+ microelectrode positioned near the cell. The cell was superfused first with the standard saline (containing 98 mM-Na^+), then a solution in which 88 mM-choline replaced an equal amount of Na^+, and finally with the original Na^+-rich solution. *A*, continuous records of Na^+ concentration (lower trace) measured by the Na^+ microelectrode and membrane current (upper trace) measured by the voltage clamp. Ionophoretic pulses produced capacitative artifacts in the Na^+ microelectrode record. Reducing external Na^+ concentration produced an upward shift in the current observed between applications of D-aspartate and reduced the current produced by D-aspartate. *B*, the amplitudes of the Na^+ current observed in the absence (□ and ◇) and presence (+ and ×) of D-aspartate are plotted as functions of Na^+ concentration. The □ and + symbols are for the traces in part *A*; the ◇ and × symbols are for similar data obtained when the same cell was superfused with a solution in which 88 mM-TEA^+ replaced an equal amount of Na^+. Membrane voltage was maintained at −70 mV.

observed when PBFI within the cell was illuminated at 360 and 400 nm (see Methods) were continuously recorded (Fig. 5*A*). The experiment began while the patch pipette was perfused with a solution containing 90 mM-K^+. Membrane voltage was ramped from −79 to 51 mV at 5·1 s intervals. The current observed during each ramp is compressed by the slow time base and appears as a vertical line whose height indicates the amplitude of an outward K^+ current. The current elicited at the time marked 1 is shown with an expanded time base in part *B*. After this trace was recorded, the regular repetition of ramps was stopped for 15·3 s and a puff of D-aspartate was applied. The response to D-aspartate is marked 2 and is shown in part *C* with an expanded time base and greater gain. Next, the patch pipette was perfused with a solution in which K^+ was replaced by choline. As the contents of the cell exchanged with the solution in the patch pipette, the fluorescence of PBFI within the cell was altered (middle trace). The internal K^+ concentration can be estimated from the fluorescence ratio (see Methods) and is plotted as the lower trace. In this case, the internal K^+ concentration declined from 90 to 9 mM. Simultaneously, outward rectification was reduced until finally little K^+ current remained (response marked 3). The regular repetition of voltage ramps was again stopped and a pulse of D-aspartate was applied. The new response to D-aspartate (marked 4) is shown in part *C* and is similar to the one (marked 2) observed at the beginning of the experiment. Subsequently, when the pipette was again perfused with the K^+-rich solution, the changes in PBFI fluorescence and outward current were reversed. In this type of experiment there are two indicators of internal K^+ concentration. First, the amplitude of the outward current indicates the internal K^+ concentration near the membrane. Second, the fluorescence of PBFI indicates the average concentration of K^+ throughout the bulk of the cytoplasm. Both measures indicate that a 10× reduction in internal K^+ concentration does not significantly affect the amplitude of the AAA-induced current (compare 2, 4 and 6). A similar result was obtained in a total of four cells. Thus, the consistent observation of an AAA-induced current in the absence of internal and external K^+ (Figs 1–4) and the supplementary experiment in Fig. 5 demonstrate that the AAA-induced current is unaffected by alterations in internal K^+ concentration.

External protons

Although monovalent cations smaller and larger than Na^+ do not readily pass through the transporter, the possibility that protons might pass deserved special consideration. Aspartate and glutamate could move as uncharged species if one carboxyl group were protonated to form a zwitterion without net charge. Erecinska, Wantorsky & Wilson (1983) have reported that protons are translocated with aspartate, whereas Gazzola *et al.* (1981) have reported that aspartate is translocated as an anion without a proton. Two series of experiments indicate that protons are not transported.

The first series of experiments measured the current induced by L-glutamate when cells were superfused with media of different pH. Glutamate was used rather than aspartate because its pK_a of 4·31 is slightly greater. The L-glutamate-induced current was measured in an external medium of pH 8·0 and then in an external medium of pH 6·2 (Fig. 6*A*). A 63-fold increase in extracellular proton concentration decreased the current approximately 15%. The pH change would increase the concentration of

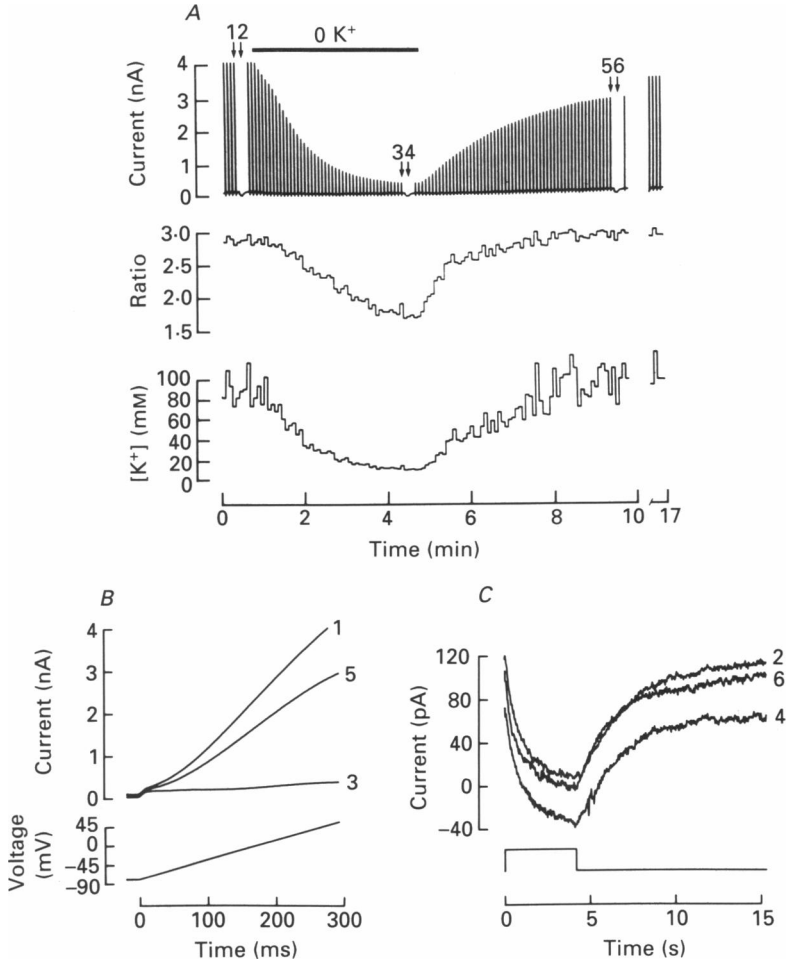

Fig. 5. AAA transport is unaffected by changes in internal K^+ concentration. *A*, continuous record on a slow time base. The patch pipette was continuously perfused first with a K^+-rich solution, next with a K^+-poor solution during the time indicated in the figure by the horizontal bar, and finally with the original K^+-rich solution. Membrane voltage was ramped at a rate of 0·44 V s^{-1} from −79 to 51 mV at 5·1 s intervals. The current recorded by the voltage clamp is the upper trace. After each ramp, the cell was illuminated for 1 s with 360 nm light and then for 1 s with 400 nm light. The ratio of the fluorescence produced by 360 and 400 nm light is plotted in the middle trace. The intracellular K^+ concentration was calculated from the ratio (see Methods) and is plotted in the lower trace. The non-linear relation between the ratio and K^+ concentration accentuates noise at high K^+ concentrations. *B*, currents elicited by voltage ramps at the times in part *A* marked 1, 3 and 5 are shown on an expanded time base. *C*, currents elicited by D-aspartate (200 μM) at the times in part *A* marked 2, 4 and 6 are shown on an expanded time base and with increased gain. The downward shift seen by comparing traces 2 and 4 may indicate that a steady outward K^+ current was partly activated at the holding voltage of −79 mV. The K^+-rich internal solution contained (in mM): KCl, 90; $(Tris)_2EGTA$, 10; $CaCl_2$, 1; Tris-HEPES, 2; PBFI, 2; pH 7·0; the K^+-poor internal solution contained (in mM): choline chloride, 90; $(Tris)_2EGTA$, 10; $CaCl_2$, 1; Tris-HEPES, 2; PBFI, 2; pH 7·0. The external medium contained (in mM): NaCl, 98; CsCl, 10; $MgCl_2$, 3·5; HEPES, 2; D-glucose, 15; TTX, 1 μM; and pH 7·4. Current records were low-pass filtered with 3 dB at 50 Hz.

protonated glutamate from 40 nM to 2·5 μM and increase the H^+ concentration from 10 to 630 nM. If protons are transported with glutamate or if glutamate is transported in the protonated form, then a rise in external proton concentration might increase influx. Instead, influx was decreased.

The second series of experiments measured intracellular pH during AAA transport. Cells were loaded with the pH-sensitive dye BCECF (Fig. 1*B*). Two puffer pipettes were positioned nearby. In one pipette 5 mM-acetate replaced 5 mM-Cl^-. In the second pipette, 200 μM-D-aspartate was added to the normal external medium. Acetate is a weak acid that in the protonated form diffuses through lipid bilayers to enter the cytoplasm and liberate a proton. Exposure to 5 mM-acetate for 1 s acidified the cytoplasm approximately 0·2 pH unit (Fig. 6*B*). Exposure to D-aspartate for 400 s did not alter intracellular pH (seven cells). The following calculation indicates that the movement of a proton with aspartate would have been detected. The dissociation constant for acetate is $1{\cdot}76 \times 10^{-5}$ M (Weast & Astle, 1981). A total concentration of 5 mM-acetate and an external pH of 7·4 produces 11·3 μM-protonated acetate. If the membrane permeability for acetate is 5×10^{-3} cm s^{-1} (J. Gutknecht, cited in Orbach & Finkelstein, 1980), then the flux of protonated acetate into a cell with a surface area of $1{\cdot}5 \times 10^{-4}$ cm^2 (equal to 150 pF capacitance, see text associated with Fig. 7) is 5×10^9 molecules s^{-1}. For comparison, if two Na^+ ions move with each AAA, a 75 pA current (a value actually smaller than the 150–220 pA observed at the resting potential, see Fig. 17) would correspond to an influx of $0{\cdot}5 \times 10^9$ AAA molecules s^{-1}. Since the duration of exposure to D-aspartate was more than 100× longer than the exposure to acetate, at least 10× more D-aspartate should have entered. Yet, the entry of aspartate did not produce a pH change. The implication is that aspartate does not provide a proton, i.e. aspartate enters as an anion without a bound proton.

External chloride

Consideration of the data in Fig. 4*B* indicated that three Na^+ ions bind at external sites. The production of an inward current requires that at least two Na^+ ions move with one AAA. A complex of three Na^+ ions and one AAA would have a charge of +2. Another possibility is for the co-ordinate movement of three Na^+ ions, one AAA, and a second anion to produce the net influx of +1 charge. The only likely second anion is Cl^-. Replacing the external Cl^- with either sulphate, a divalent anion, or isethionate, a monovalent anion of larger size, did not affect the AAA-induced current (three cells). In a separate series of five experiments, the Cl^- in the patch pipette was replaced with methanesulphonate. The AAA-induced current was similar to that observed with the normal pipette solution. Hence, Cl^- does not appear to be required for transport. If neither K^+, H^+ nor Cl^- are transported, then only Na^+ and an AAA are moved through the membrane.

Voltage dependence

Two methods for measuring the current–voltage relation of the AAA-induced current are illustrated in Fig. 7. In the first method (Fig. 7*A*), membrane potential was maintained constant and a puff of D-aspartate was delivered. The puff was repeated at each of a series of new, steady holding potentials. The amplitudes of the

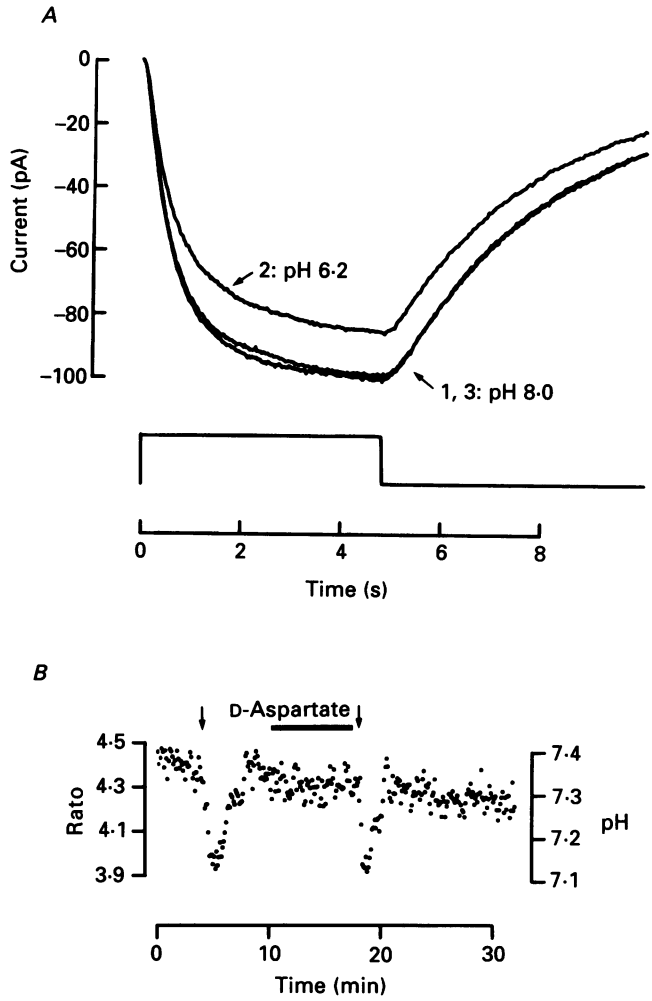

Fig. 6. Protons are not transported with an AAA. *A*, the AAA-induced current observed in media of different pH. A puff of 200 μM-L-glutamate was applied while a cell was first superfused with a medium of pH 8·0, then a similar solution of pH 6·2, and finally the original solution of pH 8·0. Increasing the external proton concentration 63 × decreased the current approximately 15%. *B*, intracellular pH is not changed during activation of AAA influx. Cells were incubated in media containing BCECF/AM and then superfused with media lacking dye. The ratio of fluorescence produced by irradiation with 440 and 500 nm light is plotted as a function of time. The ratio can be converted to intracellular pH (scale at right, see Methods). The application of a 1 s puff of medium containing 5 mM-acetate at the two times marked by the arrows decreased internal pH by 0·2–0·3 unit. A 400 s pulse of 200 μM-D-aspartate, indicated by the horizontal bar, did not alter internal pH. The external medium contained (in mM): NaCl, 106; KCl, 2; $MgCl_2$, 3·5; HEPES, 10; D-glucose, 15; pH 7·4.

AAA-induced currents are plotted as a function of membrane potential by the filled circles in Fig. 7*C*. A faster and more informative method of measuring the same relation is illustrated in Fig. 7*B*. Membrane voltage was first held constant at −70 mV and then increased at the constant rate of 0·44 V s^{-1}. The resulting current is trace 1. Next, a long puff of D-aspartate was delivered, the ramp was repeated during the puff, and the current recorded (trace 2). Subtracting the current recorded in the absence of D-aspartate from the current recorded in the presence of D-aspartate yielded the AAA-induced current as a continuous function of voltage (continuous trace in Fig. 7*C*). The method was accurate and reproducible. Repeating the procedure produced traces that superimposed (traces 3–5 in part *B*). The AAA-induced currents measured by the two methods are compared in Fig. 7*C*.

The current observed in the absence of an AAA (trace in Fig. 7*B*) allowed the passive capacitance and resistance of the membrane to be estimated. At the start of the ramp, the current stepped to a new value and then increased at an approximately linear rate. The initial step is the capacitative current, $i = C\mathrm{d}V/\mathrm{d}t$. The rate of linear increase is determined by the resistance according to the equation $R = \Delta V/\Delta i$. In a series of sixty-two cells the capacitance was 150±64 pF (mean±S.D.) and the resistance was 3·35±1·37 GΩ (note that K^+ currents were blocked by deleting K^+ from the internal and external solutions and including Cs^+ in both solutions).

It will be useful to have a simple, quantitative description of how voltage affects the current produced by transporter activity. A measurement of the AAA-induced current over an extended voltage range is shown in Fig. 8. In this case, the AAA-induced current was measured when the membrane potential was first ramped upwards and then downwards from a voltage of −54 mV and the two limbs of the complete curve pieced together. The shape of the entire curve can be described by the equation

$$I = B\exp(-\beta V/\zeta) + C, \tag{3}$$

where B, C and β are coefficients and $\zeta = 25{\cdot}4$ mV ($\zeta = RT/zF$ where R is the gas constant, T is absolute temperature, F is Faraday's constant, and z is valency). In a series of sixty-two cells the value of β was 0·60±0·03 (mean±S.D.). The values of both B and C depended on the internal and external Na^+ concentrations (see below, Fig. 13 and associated text).

Binding sites do not move in the membrane

A carrier is sometimes modelled as a binding site that moves back and forth through a membrane. Substrates are assumed to occupy and move with the binding site. If the substrate is charged, then binding of the substrate changes the net charge moving through the membrane. In this situation, the amount of time the binding site spends on each side of the membrane depends on both membrane potential and substrate concentration. As a consequence, the shape of the current–voltage relation would depend upon substrate concentration.

The shape of the current–voltage relation for the current produced by D-aspartate was independent of D-aspartate concentration (Fig. 9). The current–voltage relations for two concentrations of external D-aspartate are shown in Fig. 9*A*. After rescaling, the two curves coincide (Fig. 9*B*) demonstrating that the shape of the current–voltage relation is not affected by external AAA concentration. This simple observation leads to the important conclusion that the coefficient $K_{\text{D-Asp}}$ does not

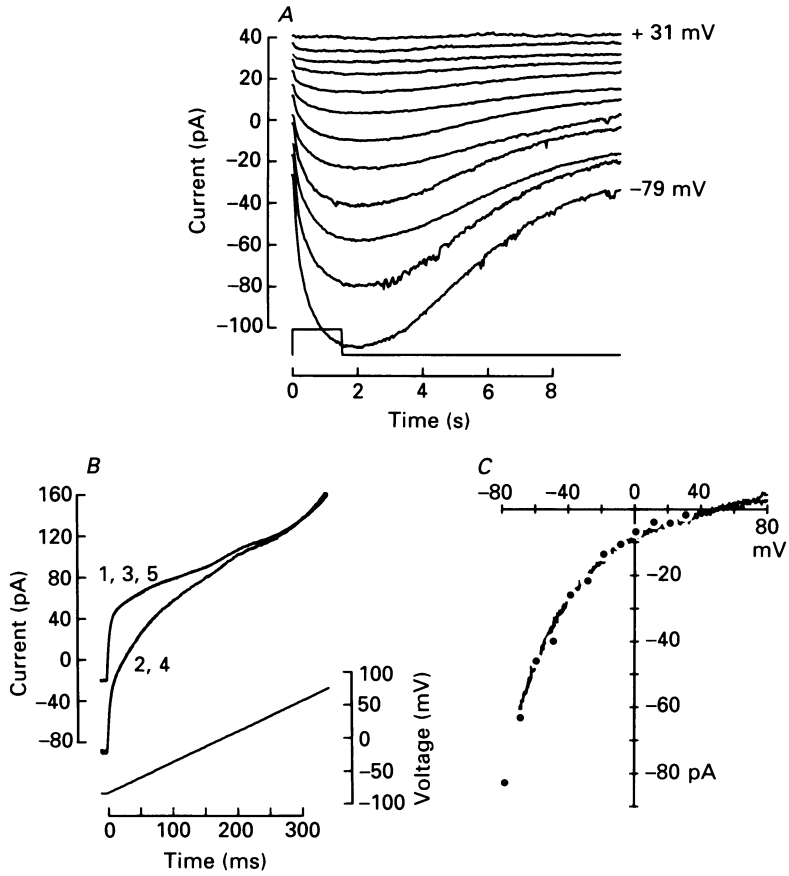

Fig. 7. Two methods for measuring the current–voltage relation of the AAA-induced current. All the data are from one cell. *A*, membrane potential was maintained at one of twelve values and current was recorded during a puff of 20 μM-D-aspartate whose duration is indicated by the timing trace. The potential was changed from −79 to +31 mV in 10 mV steps. The largest response was observed at −79 mV and successively smaller currents were observed at more depolarized potentials. *B*, membrane potential was increased from −70 to +80 mV at 0·44 V s^{-1} and membrane current recorded (trace 1). Next, a long puff of D-aspartate was delivered, the ramp repeated, and membrane current again recorded (trace 2). The difference between traces 1 and 2 is the AAA-induced current. The procedure was repeated without (trace 3), with (trace 4) and without (trace 5) D-aspartate. Traces 1, 3 and 5 superimpose; and, traces 2 and 4 superimpose. *C*, comparison of current–voltage relations for the D-aspartate-induced current determined by the methods in parts *A* and *B*. Symbols are from part *A*. Continuous traces are from part *B* (calculated by subtracting trace 1 from 2, and trace 3 from 4). The two continuous traces superimpose. The sequence for completing the experiment was: traces 1 and 2, then the responses of part *A*, and finally traces 3, 4 and 5. Membrane capacitance and resistance can be estimated from traces 1, 3 and 5 in part *B*. The current step at the onset of the ramp indicates a capacitance of 161 pF; the slope of the current change produced as the voltage was ramped from −70 to 0 mV indicates a resistance of 1·8 GΩ.

depend upon membrane voltage. Consequently, voltage does not affect binding and the binding site does not sense the voltage field. Binding and transport are separate events. The amplitude of the current can be predicted by the product of (i) a Michaelis equation that describes the quantity of substrate that occupies a binding site and (ii) a transport equation that describes the rate at which bound substrate is moved through the membrane. The shape of the current–voltage relation for the AAA transporter does not depend upon substrate concentration (Fig. 9). Consequently, the mobile binding-site model must be abandoned for AAA transport.

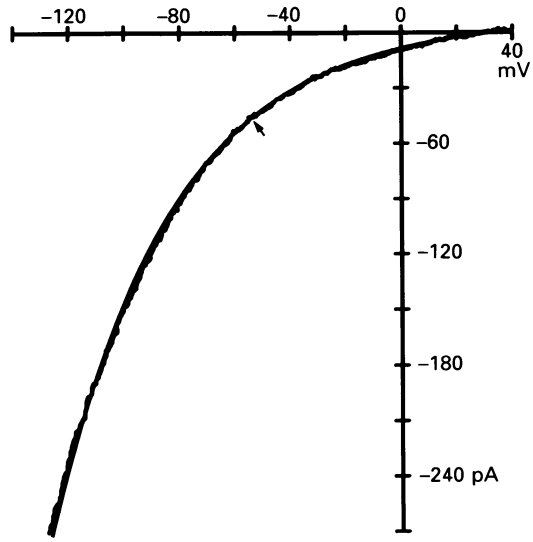

Fig. 8. The current–voltage relation of the AAA-induced current measured over an extended voltage range. The procedure in Fig. 7*B* was modified. Membrane voltage was ramped upwards and then downwards from −54 mV (indicated by the arrow). Current–voltage relations were recorded in the standard saline and in a similar solution containing 200 μM-D-aspartate. The AAA-induced current is compared with the prediction of eqn (3) with $\beta = 0{\cdot}57$, $B = -17{\cdot}22$ pA and $C = 7{\cdot}56$ pA. The calculated curve superimposes over the observed current.

Efflux is electroneutral

Simple models often assume that the operation of carriers is completely reversible and that the mechanism for influx is the same as the mechanism for efflux. The preceding experiments demonstrate that external L-glutamate or D- or L-aspartate induce a current (Fig. 2*A*). The following experiments demonstrate that internal L-glutamate or D-aspartate do not induce a current. Thus, there must be an asymmetry in the mechanisms of influx and efflux.

Membrane current was recorded while the patch pipette was continuously perfused with a solution lacking L-glutamate. Current–voltage relations were determined before and during exposure to external D-aspartate. The AAA-induced current is trace 2 in Fig. 10*B*. Next, the pipette was perfused with a solution containing 30 mM-L-glutamate, the current–voltage relations were again determined before and during exposure to external D-aspartate, and the AAA-induced current was calculated

(trace 4). Finally, the pipette was again perfused with the glutamate-free solution, the current–voltage relations measured a final time, and the AAA-induced current calculated (trace 6). The introduction of 30 mM-L-glutamate into the cell did not itself produce a current (Fig. 10*A*, traces 1, 3 and 5). However, internal L-glutamate

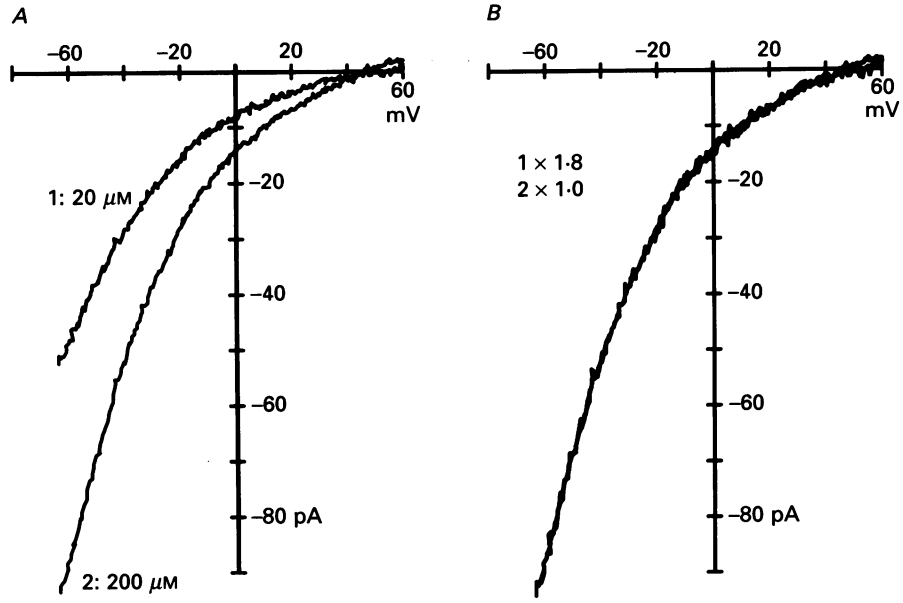

Fig. 9. The shape of the current–voltage relation is independent of external D-aspartate concentration. Two puffer pipettes containing 20 and 200 μM-D-aspartate were positioned near a glial cell. *A*, the current–voltage relation for the AAA-induced current was determined for each concentration as described in Fig. 7*B* and *C*. *B*, the two curves of part *A* superimpose after the current produced by 20 μM is multiplied by 1·80.

decreased the current induced by external D-aspartate (Fig. 10*B*, compare trace 4 with traces 2 and 6). Similar results were obtained in four experiments in which L-glutamate was introduced into a cell and in six experiments in which D-aspartate was introduced into a cell by perfusing the patch pipette. The ability of internal L-glutamate or D-aspartate to decrease the current normally elicited by external D-aspartate may be termed *trans*-inhibition.

Although internal L-glutamate does not produce a membrane current, the following experiment demonstrates that glutamate does efflux. The ability of L-glutamate to be transported out of a glial cell was studied with a fluorescence assay. Glutamate dehydrogenase (GDH) is a commercially available enzyme that couples the oxidation of L-glutamate to the reduction of NADP (or NAD):

$$\text{L-glutamate} + \text{NADP}^+ + \text{H}_2\text{O} \rightarrow \alpha\text{-oxoglutarate} + \text{NADPH} + \text{NH}_4^+.$$

The reactant NADP is not fluorescent, whereas the product NADPH is fluorescent. If cells are bathed in GDH and $NADP^+$ and irradiated with 360 nm light, the release of L-glutamate generates blue light. The volume around a cell was reduced by an overlay of perfluorinated oil (see Methods). Fluorescence became detectable when the extracellular volume was sufficiently small. Membrane potential was controlled with

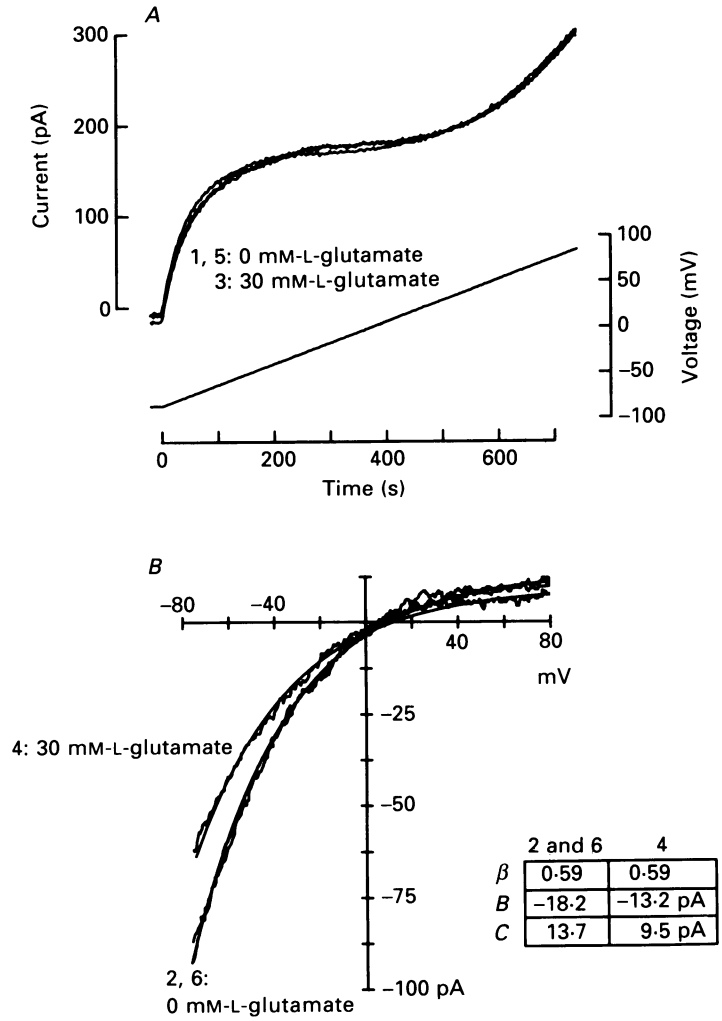

Fig. 10. Internal L-glutamate does not itself produce a current but inhibits the current induced by external D-aspartate. Membrane current was recorded while a patch pipette was continuously perfused first with a glutamate-free saline (in mM: NaCl, 30; TEA-Cl, 60; Na_2EGTA, 10; $CaCl_2$, 1; HEPES, 2), next with a solution containing 30 mM-L-glutamate substituted for an equal amount of Cl^-, and finally with the original glutamate-free solution. Membrane voltage was ramped from −85 to 85 mV. *A*, current–voltage relations for membrane currents recorded while the cell was superfused with the standard saline and the pipette was perfused with glutamate-free (traces 1 and 5) and glutamate-rich (trace 3) solutions. *B*, current–voltage relations for the current induced by 20 μM-external D-aspartate in the absence (traces 2 and 6) and presence (trace 4) of 30 mM-internal L-glutamate. Introducing internal L-glutamate did not change the current–voltage relation observed while the cell was bathed in saline (part *A*) but decreased the current induced by external D-aspartate (part *B*). The current–voltage relations for the AAA-induced currents can be described by eqn (3). Values of β, B and C are given in the inset. Introducing 30 mM-internal L-glutamate reduced B and C but did not change β.

a whole-cell voltage clamp. The patch pipette that communicated with the cell interior contained 30 mM-sodium L-glutamate. At 30 s intervals, membrane voltage was stepped to a new level. The relation between membrane voltage and current is plotted in the upper panel of Fig. 11; the relation between membrane voltage and fluorescence is plotted in the lower panel of Fig. 11. Fluorescence was detected at −90 mV and increased as the cell was depolarized. A similar result was obtained from three additional cells, in which, however, the size of the fluorescent signal was smaller, perhaps because the extracellular volume trapped by the oil was larger. The fluorescent signal is not a simple measure of efflux rate, but is determined by efflux, reuptake, the volume of the extracellular space, the duration of a voltage step, and the efficiency of the enzyme. It has therefore not been possible to derive from the fluorescent signal the relation between voltage and efflux rate. None the less, qualitative statements are possible. A fluorescent signal observed between −90 and +30 mV indicates that efflux occurs throughout this range. However, the increase in fluorescence at depolarized potentials need not indicate that efflux is voltage dependent. Instead, an increase in fluorescence might occur if influx ceases (as predicted by the results in Figs 7–9) and efflux operates unopposed. Thus, the result in Fig. 11 indicates that efflux operates over a wide voltage range but does not allow the voltage dependence for efflux to be estimated. The previous result of Fig. 10 demonstrates that neither intracellular L-glutamate nor D-aspartate produces a current. The combined results of Figs 10 and 11 indicate that efflux occurs over a wide voltage range without the production of a current.

Transcoupling

The enzyme GDH is specific for L-glutamate and does not recognize D-aspartate. Therefore, it was possible to continue the experiment illustrated in Fig. 11 and to measure the effect of external D-aspartate on the release of L-glutamate. D-Aspartate was ionophoresed from a micropipette positioned near the cell. As expected, the application of external D-aspartate produced a membrane current (upper panel of Fig. 11). The simultaneously measured relation between membrane potential and fluorescence is plotted in the lower panel of Fig. 11. Greater fluorescence now occurred at hyperpolarized potentials and less fluorescence occurred at depolarized potentials. Thus, an external AAA produced a current and altered the efflux of L-glutamate. A parsimonious explanation for an interaction between influx and efflux is that both are mediated by the same transporter. The augmented fluorescence at hyperpolarized potentials may be termed *trans*-stimulation and the diminished fluorescence at depolarized potentials may be termed *trans*-inhibition. External AAA produces a *trans*-inhibition at depolarized voltages, where the inward movement of AAA ceases, but a *trans*-stimulation at hyperpolarized voltages, where a large electrogenic influx of AAA develops (see Figs 7–9). In contrast, Fig. 10*B* demonstrates *trans*-inhibition by an internal amino acid at all voltages. A simple model that accounts for these phenomena will be presented in the Discussion.

Two Na^+-dependent currents

Figure 4 demonstrates that Na^+ carries both a current in the absence of an AAA and is co-transported during AAA influx. An appreciation of the relationship

between the two Na^+-dependent currents can be obtained from Fig. 12. Current–voltage relationships were measured while a cell was superfused with first a Na^+-free medium (choline was the principal cation), then a Na^+-rich medium, and finally a Na^+-rich medium with 200 μM-D-aspartate. Subtracting the current recorded

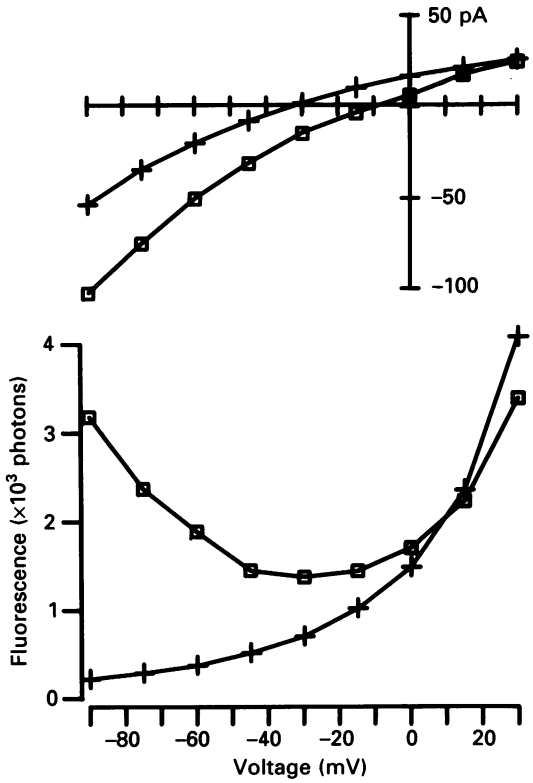

Fig. 11. Efflux of L-glutamate detected with a fluorescence assay. The extracellular solution contained 1 mg ml^{-1} glutamate dehydrogenase, 2 mM-NADP and 2 mM-ADP added to a medium containing (in mM): NaCl, 98; CsCl, 10; $MgCl_2$, 3·5; phosphate buffer, 2; pH 7·4. The volume of the external solution was reduced by an overlay of perfluorinated oil (see Methods). Fluorescence and membrane current were measured during a series of 30 s voltage steps (+). Afterwards, D-aspartate was continuously ejected from a nearby ionophoretic pipette and the procedure repeated (□). The patch pipette contained (in mM): sodium L-glutamate, 30; TEA-Cl, 60; Na_2EGTA, 10; $CaCl_2$, 1; HEPES, 2. The minimum slope of the current–voltage relation is equivalent to a resistance of 2·7 GΩ. This represents the parallel combination of the membrane and seal resistance. Consequently, the resistance of the seal must have been considerably higher and little L-glutamate could have leaked across the seal between the pipette and the membrane.

in the Na^+-free medium from the currents recorded in Na^+-rich media yielded the result of Fig. 12*A*. Na^+ alone produced a current (trace 1). Na^+ and an AAA together produced a larger current with a different voltage dependence (trace 2). The difference between the two traces in part *A* is the AAA-induced current shown in part *B* (comparable to Fig. 7*C* and Fig. 8). The two Na^+-dependent currents observed in Fig. 12 are described in greater detail in the following two sections: first, sodium's

role in the AAA-induced current; second, the current carried by Na^+ in the absence of an AAA (as an uncoupled Na^+ current).

Na^+ co-transport. The shape of the current–voltage relation has been described by eqn (3). An important feature, upon which we have not previously commented, is a

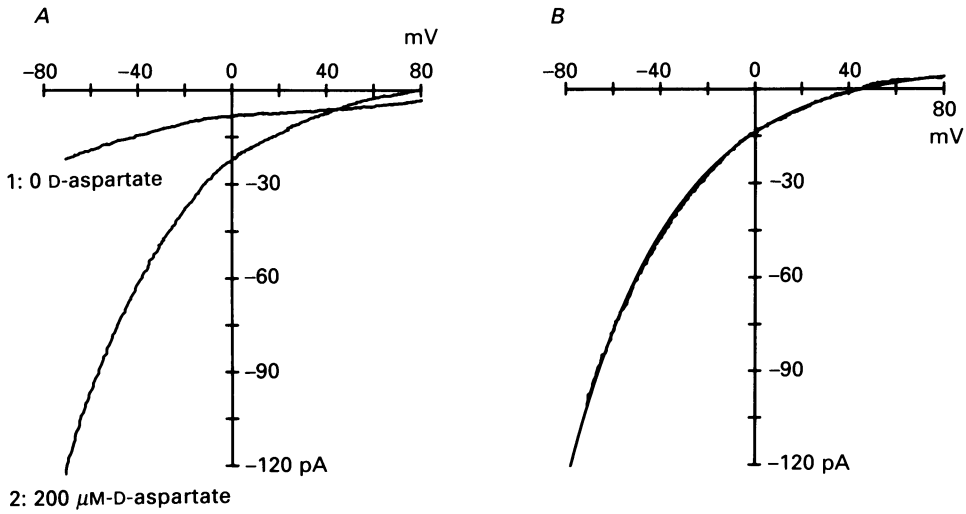

Fig. 12. Current–voltage relations for two Na^+-dependent currents. Current–voltage relations were measured while a cell was superfused with first a Na^+-free medium (choline was the principal cation), then a Na^+-rich medium, and finally a Na^+-rich medium with added 200 μM-D-aspartate. *A*, subtracting the current recorded in the Na^+-free medium from the current recorded in the Na^+-rich medium yielded trace 1. Subtracting the current recorded in the Na^+-free medium from the current recorded in the medium containing Na^+ and 200 μM-D-aspartate yielded trace 2. *B*, the difference between traces 1 and 2 of part *A* is compared with the prediction of eqn (3) with $\beta = 0{\cdot}57$, $B = -22{\cdot}45$ pA and $C = 7{\cdot}22$ pA.

small outward current at depolarized potentials (see Fig. 12*B*). It is a *bona fide* part of the current–voltage relation. This feature enters into eqn (3) as the value of C. Indeed, eqn (3) describes the total current induced by an external AAA as the sum of an inward and an outward component. Experiments in which the external or internal Na concentration were altered indicate that this mathematical formulation, which describes the total current as the sum of two components, may have a functional basis. The current–voltage relations for the AAA-induced current at three external Na^+ concentrations are shown in Fig. 13*A*. Each curve has a null potential at which the current is zero. Increasing the external Na^+ concentration shifted the null potential to a more positive voltage. The shift in null potential immediately demonstrates that each curve has a different shape. The change in shape can be quantitatively described with the aid of eqn (3). Increasing the Na^+ concentration increased B and decreased C without markedly affecting β. That is, a change in Na^+ concentration changed the relative contribution of each term without altering the voltage dependence of the individual terms. A similar change was observed in each of six cells in which the experiment was attempted.

Internal Na^+ concentration was altered during the course of an experiment by

changing the solution within the patch pipette. First, the patch pipette was continuously perfused with a solution lacking Na^+. Current–voltage relations were determined before and during exposure to external D-aspartate, and the AAA-induced current calculated (trace 1 in Fig. 13*B*). Next, the pipette was perfused with a solution containing 80 mM-Na^+, the current–voltage relations again determined before and during exposure to external D-aspartate, and the AAA-induced current calculated (trace 2). The introduction of 80 mM-Na^+ altered the voltage dependence of the aspartate-induced current. The change can be described with the use of eqn (3). The introduction of Na^+ increased C from 5·93 to 13·3 pA and decreased B from −18·7 to −14·5 pA. A similar change was observed in each of five cells in which the experiment was attempted. Thus, the experiment illustrated in Fig. 13*A* demonstrates that external Na^+ increased B and decreased C; the experiment illustrated in Fig. 13*B* demonstrates that internal Na^+ has the opposite effect.

Although experiments like that in Fig. 13 demonstrate that C is increased when the external Na^+ concentration is decreased from 98 to 29 mM, one caveat is necessary. Further reducing the Na^+ concentration does not continue to increase C. Indeed, when the external Na^+ concentration is reduced to zero, an AAA does not produce a current, not even an outward component. A possible interpretation is that Na^+ efflux is facilitated when one or two Na^+ ions and an AAA bind to the external surface, but ceases if either all of the external Na^+ binding sites are empty or if all three of the external Na^+ binding sites are occupied. A simple model that accounts for these phenomena will be presented in the Discussion.

Uncoupled Na^+ current. Na^+ might be able to move through the transporter even without the co-transport of an amino acid. The movement of Na^+ alone would represent a slippage or leakage in the coupling of Na^+ to AAA transport. Suggestive evidence for this view comes first from experiments with Li^+, an ion that usually permeates Na^+-selective pores even better than Na^+ but does not efficiently pass through carriers. Indeed, the inability of Li^+ to substitute for Na^+ was one of the criteria used to identify a carrier-mediated current. We have already commented that substituting Li^+ for Na^+ produced an apparent outward current (seen in Fig. 2*C* as the upward shift of trace 2; a similar behaviour is seen in Fig. 4*A* when Na^+ was replaced with either choline or TEA^+). More complete information is provided in Fig. 14*A*. Current–voltage relations were measured in media containing choline, Li^+ and Na^+. If choline does not carry an inward current, then the currents carried by Li^+ and Na^+ can be estimated and compared. The results in Fig. 14*A* demonstrate that Li^+ is a poor substitute for Na^+. The dependence of the uncoupled current on external Na^+ can be determined from the data in Fig. 4*A* and is plotted by the diamonds and squares in Fig. 4*B*. Because the current produced by removing Na^+ was only approximately one-tenth the size of the maximum AAA-induced current, the data are noisy and it was difficult to determine the exact dependence on Na^+ concentration. None the less, the apparent sigmoid increase in amplitude produced by an increase in Na^+ concentration indicates that more than one Na^+ ion interact at the external surface. The data in Fig. 4*B* have been fitted with eqn (2) using $n = 3$, $K_{Na} = 88$ mM and $I_{max} = 18{\cdot}2$ pA. Similar values were obtained from two additional cells.

The shape of the current–voltage relation for the uncoupled Na^+ current was

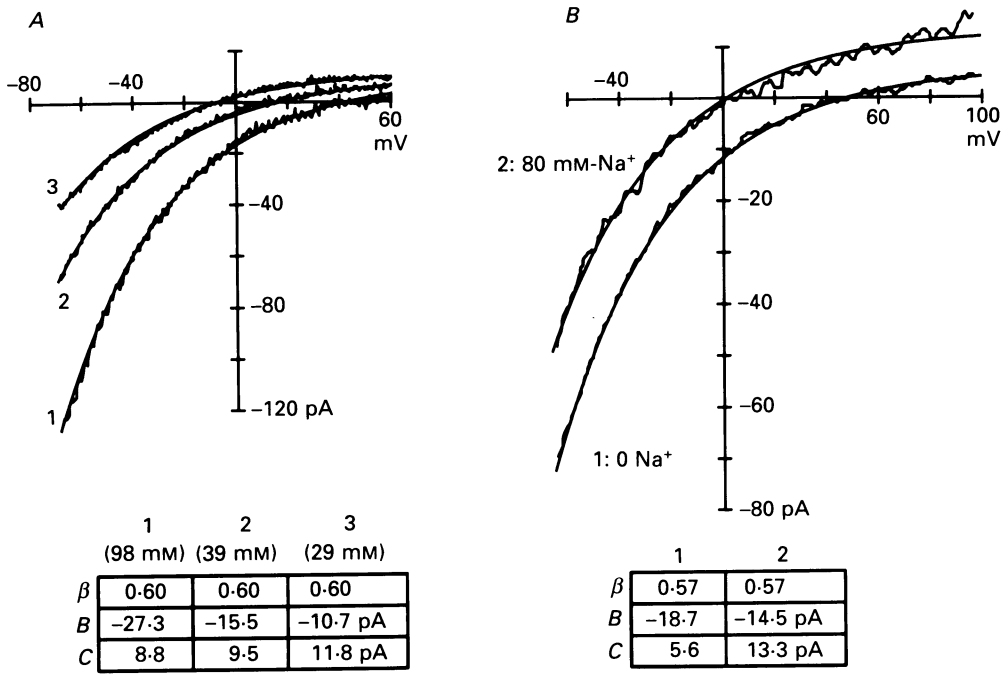

	1 (98 mM)	2 (39 mM)	3 (29 mM)
β	0·60	0·60	0·60
B	-27·3	-15·5	-10·7 pA
C	8·8	9·5	11·8 pA

	1	2
β	0·57	0·57
B	-18·7	-14·5 pA
C	5·6	13·3 pA

Fig. 13. Changing external or internal Na^+ concentration changed the shape of the current–voltage relation for the AAA-induced current. *A*, changing external Na^+ concentration. The cell was superfused sequentially with solutions containing 98 mM-Na^+, 39 mM-Na^+ and 29 mM-Na^+ (Na^+ was replaced with choline). An ionophoretic pipette containing D-aspartate was positioned near the cell; current–voltage relations were measured before and during the application of D-aspartate; and the AAA-induced current was calculated for each Na^+ concentration. The three current–voltage relations for the AAA-induced current (trace 1 is 98 mM, 2 is 39 mM and 3 is 29 mM) have different null potentials. Each relation can be described by eqn (3). Values of β, B and C are given in the inset. *B*, changing internal Na^+ concentration. The patch pipette was continuously perfused with a Na^+-free solution (in mM: TEA-Cl, 90; TEA_2EGTA, 10; $CaCl_2$, 1; HEPES, 2). Current–voltage relations were determined before and during exposure to a puff of 200 μM-D-aspartate. The AAA-induced current is trace 1. Next, the pipette was perfused with a solution in which 80 mM-Na^+ replaced an equal amount of TEA^+. Current–voltage relations were again determined before and during exposure to external D-aspartate and the AAA-induced current calculated (trace 2). Each relation can be described by eqn (3). Values of β, B and C are given in the inset.

independent of Na^+ concentration. The current–voltage relations for two concentrations are shown in Fig. 14*B*. After rescaling, the two curves coincide (Fig. 14*C*). Thus, the amplitude of the uncoupled Na^+ current can be predicted by the product of a term that describes Na^+ binding (eqn (2)) and a term that describes the rate at which bound Na^+ is moved through the membrane.

The uncoupled Na^+ current was similar to the AAA-induced current in four respects. (i) The current required Na^+ and was poorly carried by Li^+. (ii) The relation between external Na^+ concentration and current amplitude was described by eqn (2) with n equal to 2 or 3, indicating multiple Na^+ binding sites. (iii) Na^+ binds at the

membrane surface outside the voltage field. (iv) Binding is rapid and the subsequent movement of charge through the membrane is rate limiting. These similarities suggest that the uncoupled Na^+ current may be produced by the 'leakage' of Na^+ through a co-transport carrier. Of course, Müller cells may have several different Na^+

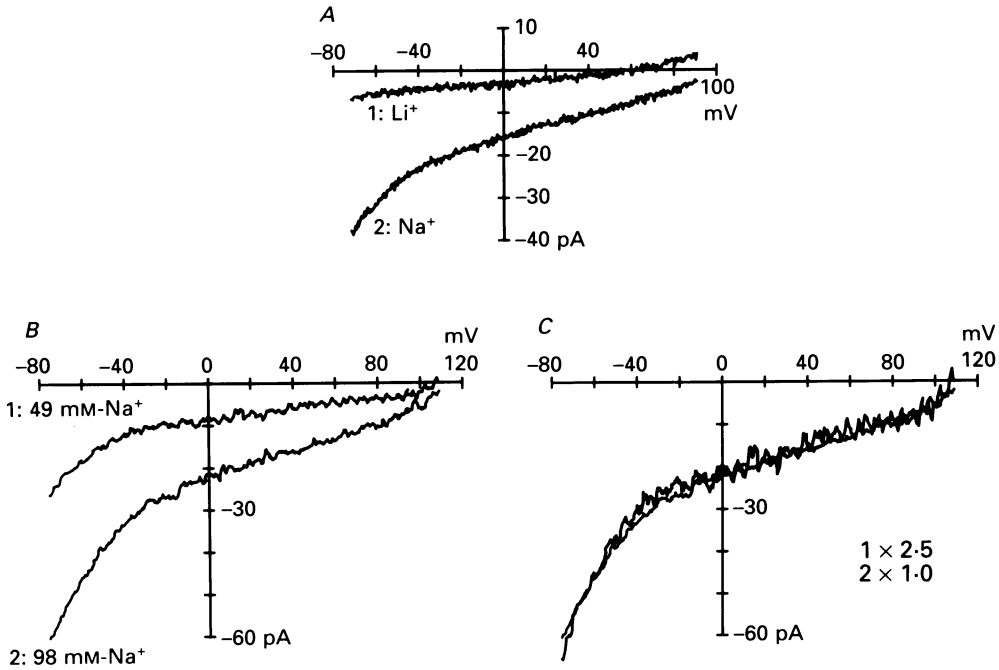

Fig. 14. Na^+ enters in the absence of external AAA. *A*, Li^+ is a poor substitute for Na^+ in carrying the uncoupled current. A cell was superfused with solutions containing choline, Li^+, choline, Na^+ and finally choline (all 98 mM). The current–voltage relation was measured in each solution. Subtracting the current recorded in choline from the current recorded in Li^+ yielded trace 1. Subtracting the current recorded in choline from the current recorded in Na^+ yielded trace 2. *B*, current–voltage relations for the uncoupled current measured at two concentrations of external Na^+. The cell was superfused first with a solution containing 98 mM-choline, next a mixture of 49 mM-choline and 49 mM-Na^+, then 98 mM-choline, and finally 98 mM-Na^+. During exposure to each solution, the voltage was ramped from −75 to 110 mV and the current–voltage relation measured. The difference between the relation measured before and during exposure to 49 mM-Na^+ is trace 1; the difference between the relation measured before and during exposure to 98 mM-Na^+ is trace 2. *C*, the shape of the current–voltage relation for the uncoupled current is independent of the external Na^+ concentration. The two curves of part *B* superimpose after trace 1 is multiplied by 2·5.

co-transport carriers. The large size of the AAA-induced current may indicate that the AAA transporter is relatively abundant. In that case, the uncoupled Na^+ current would flow primarily through the AAA transporter.

Na^+ leakage provides an easy explanation for the outward current induced by an external AAA at depolarized potentials. In the absence of an AAA, Na^+ leaks through the transporter. Leakage has only a shallow dependence on membrane voltage and produces a relatively flat current–voltage relation between 0 and 80 mV.

An external AAA occupies the transporter and produces a current composed of two components: one component is due to the cessation of Na^+ leakage; the other component is due to the initiation of a current created by the inward movement of Na^+ and an AAA. A model which accounts for leakage, co-transport, and their

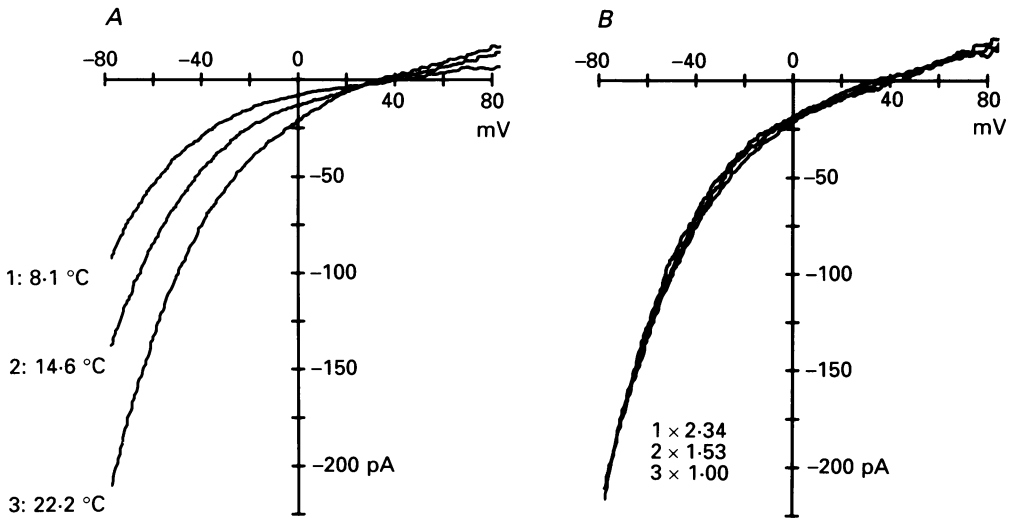

Fig. 15. Current–voltage relations for the AAA-induced current at three different temperatures. The cell was superfused with a solution whose temperature was controlled by a Peltier device. The temperature within 100 μm of a cell was recorded by a miniature thermocouple. D-Aspartate (400 μM) was delivered from a puffer pipette. *A*, the current–voltage relation for the AAA-induced current was determined at 8·1, 14·6 and 22·2 °C. *B*, the curves of part *A* superimpose after they are rescaled. The trace recorded at 8·1 °C is multiplied × 2·34 and the trace recorded at 14·6 °C is multiplied × 1·53.

interaction will be presented in the Discussion. The ability to explain the shape of the current–voltage relation, including an outward component at depolarized voltage, is an additional reason for suggesting that leakage and co-transport are mediated by the same transporter.

Kinetics of transport

Kinetic properties of the transport pathway can be deduced by recording the current at different temperatures and observing the current following rapid changes in external AAA concentration.

Temperature dependence

Cells were superfused with a solution whose temperature was controlled by a Peltier device. The temperature was recorded by a miniature thermister positioned within 100 μm of a cell. D-Aspartate (400 μM) was delivered from a puffer pipette. Raising the temperature increased the AAA-induced current (Fig. 15*A*). The current–voltage curves observed at different temperatures all had the same shape

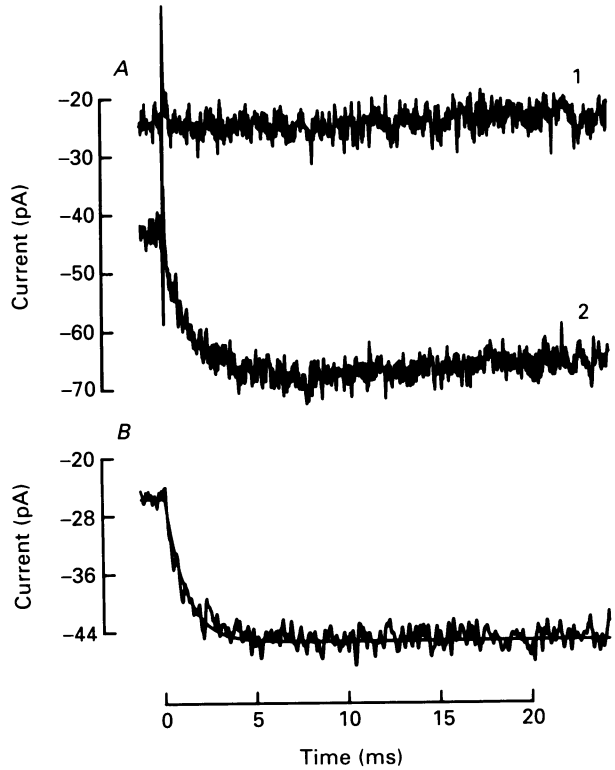

Fig. 16. *A*, response to a concentration jump produced by the photolysis of caged L-glutamate. First, a cell was bathed in saline (trace 1). The flash of a xenon lamp produced a brief event at the moment it was triggered but did not produce a sustained current. Next, 4 mM-caged L-glutamate was puffed continuously over the cell (trace 2). A steady inward current (indicated by the difference between the initial levels of traces 1 and 2) may be due to a small amount of free glutamate. The flash of a xenon lamp produced an inward current that rose to a maximum in less than 5 ms. *B*, the recording resolution of the patch clamp system. A 20 pA current was capacitatively injected at the input of the recording amplifier. The rise of the current can be described by a single exponential. The smooth line plots the rise of an exponential with a time constant of 1·07 ms. Data were low-pass filtered with 3 dB attenuation at 4 kHz and digitized at 20 kHz. Each trace in part *A* is the average of four responses; the trace in part *B* is the average of sixteen responses. The display scales for parts *A* and *B* have been adjusted so that the records are easily compared. Membrane voltage was maintained at −66 mV. The temperature was 24·5 °C.

and could be superimposed (Fig. 15*B*) if the smaller amplitude curves were each multiplied by a scaling factor, Q. The value of Q depended up the change in temperature, ΔT. A series of experiments may be compared by defining a Q_{10},

$$Q_{10} = \exp[(10/\Delta T)\ln Q], \tag{4}$$

where ΔT is different for each experiment. In six cells the Q_{10} was $1{\cdot}95 \pm 0{\cdot}16$ (mean $\pm$ S.D.). The observed Q_{10} of less than two indicates that a large conformation change did not occur.

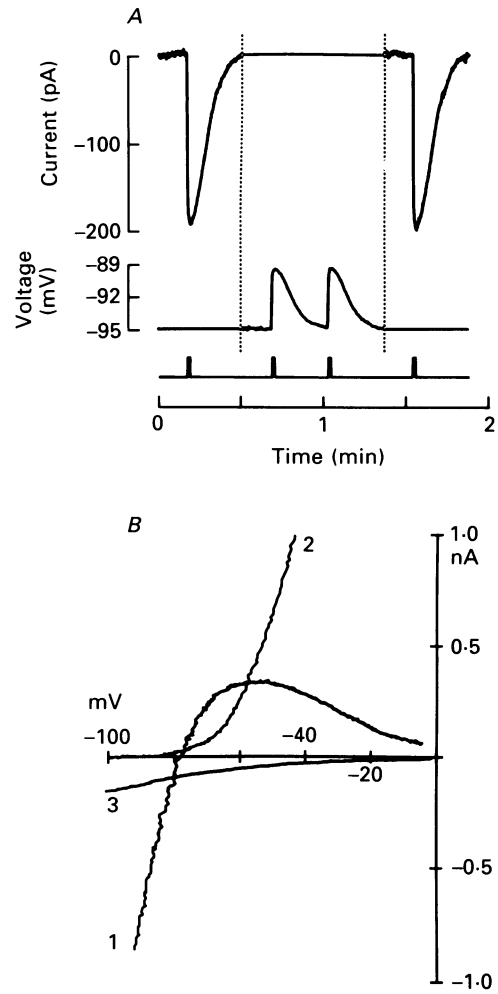

Fig. 17. *A*, the AAA-induced current produces a modest voltage response during physiological conditions. The voltage clamp was adjusted for zero holding current at a resting potential of −94·8 mV. A puff of 200 μM-D-aspartate from a nearby pipette produced a 195 pA response. Next, the voltage clamp was switched (at the first dotted line) to include a feedback circuit that maintained zero injected current and thus allowed the voltage to change. Two puffs of D-aspartate each produced a 5·5 mV depolarization. Finally, voltage-clamp recording resumed (at the second dotted line) and a final puff of D-aspartate was applied. Activation of the AAA transporter produced a 195 pA current or a 5·5 mV depolarization. A 10 mV step from the resting potential indicated an input impedance of 34 MΩ. The patch pipette contained (in mM): KCl, 90; K_2EGTA, 10; $CaCl_2$, 1; HEPES, 2; and pH 7·4. The extracellular solution contained (in mM): NaCl, 106; KCl, 2; $MgCl_2$, 3·5; $CaCl_2$, 2, HEPES, 2; glucose, 15. *B*, the membrane potential of a Müller cell is determined primarily by K^+ currents. The patch pipette was perfused with a solution containing 98 mM-K^+ and membrane current was recorded while the cell was superfused first with a solution containing 5 mM-K^+ and then a K^+-free solution containing 5 mM-Cs^+. The difference, produced by replacing external K^+ with Cs^+, is an inwardly rectifying K^+ current (trace 1). Next, the patch pipette was perfused with a solution containing 98 mM-TEA^+. An outwardly rectifying K^+ current (trace 2) was blocked by replacing internal K^+ with TEA^+. Finally, the cell was exposed to 200 μM-D-aspartate. The AAA-induced current (trace 3) is smaller than either the inwardly or outwardly rectifying K^+ currents. Traces have been corrected for the series resistance of the patch pipette.

A Q_{10} of 1·95 may be compared to a value of 1·2 for free aqueous diffusion, 1·3–1·4 for diffusion through an open pore, and approximately 3 for the rate constants describing the gating of voltage-activated Na^+ and K^+ pores (Frankenhaeuser & Moore, 1963). The Q_{10} can be used to estimate the height of an energy barrier, G, which must be traversed during influx:

$$G = RT[(T+10)/10]\ln Q_{10}, \tag{5}$$

where R is the gas constant and T is absolute temperature. The energy barrier can be related to a rate constant, α, defined by an equation with the same form as the first term of eqn (3). The second term, C, which makes a small contribution at hyperpolarized potentials and when the internal Na^+ concentration is low, can be ignored to simplify the analysis:

$$\alpha = (\nu kT/h)e^{-(G+\beta V)/RT}, \tag{6}$$

where β and V have the same meaning as in eqn (3), ν is a probability factor that is less than 1, k is Boltzmann's constant, and h is Planck's constant ($kT/h = 6{\cdot}1 \times 10^{12}\ s^{-1}$ at 20 °C). The value of ν is not known; assuming a value of 1 allows an upper estimate for the rate constant. A Q_{10} of 1·95 implies an energy barrier of 11 kcal mol^{-1} and a rate constant (at −70 mV and 20 °C) of $10^4\ s^{-1}$ (or, if each translocation moves one charge, a time constant of 100 μs). This is equivalent to each transport molecule producing a steady current of 1·6 fA. Since the maximum AAA-induced current at −70 mV is approximately 200 pA, a cell would require $1{\cdot}2 \times 10^5$ transport molecules. Because the binding of substrate is not rate limiting for the production of current (Fig. 8), the energy barrier of 11 kcal mol^{-1} is associated with translocation. Furthermore, binding sites do not move within the membrane's voltage field (Fig. 9 and associated text). Hence, translocation is associated with an energy barrier of 11 kcal mol^{-1} that does not involve a conformational change.

The above calculations indicate that 20 μM-D-aspartate (the half-saturating concentration) produces a continuous flux of 5×10^3 aspartate molecules s^{-1} through each transport molecule. Can an AAA diffuse to the transporter fast enough to support this rate of influx? Fick's law of diffusion describes the rate at which new AAA molecules arrive at the external binding site. The maximum flux, Φ, that can diffuse to the binding site is (Moore & Pearson, 1981)

$$\Phi = 2\pi\rho Dc, \tag{7}$$

where ρ is the cross-sectional capture radius of the binding site, D is the diffusion constant, and c is concentration. If ρ is 1 nm and D is $1{\cdot}5 \times 10^{-5}\ cm^2\ s^{-1}$, then $\Phi = 10^5$ ions s^{-1}. This number might be increased slightly by electrostatic interactions that assist in attracting a negatively charged AAA into a binding site that already contains positively charged Na^+ ions. Thus, an AAA diffuses to a binding site at least 10× faster than it passes through the transporter. On the whole the calculations provide order-of-magnitude estimates that confirm that the movement of AAA to the membrane is not a rate-limiting step and that the movement of an AAA and two Na^+ ions through the membrane can produce the observed current amplitude. In contrast, it may be noted in passing that protonated aspartate (see section above titled *External protons*) is not sufficiently abundant to support the observed flux.

Concentration jump

The maximum rate of influx may be determined by observing the time course of the current initiated by a quick increase in extracellular AAA concentration. The photolysis of a photo-labile derivative of L-glutamate was used to produce a jump in concentration that was complete in less than 1 ms. Initially a cell was bathed in the standard saline. During this time a flash of light from a xenon lamp did not produce a membrane current (Fig. 16*A*, trace 1). Next, a medium containing 4 mM-caged glutamate was puffed continuously over the cell (trace 2). Continuous exposure to caged L-glutamate produced a steady inward current (note the shift between traces 1 and 2). The steady inward current could have been produced by a small amount of free L-glutamate (i.e. if the ratio of free glutamate to caged glutamate was approximately 1:1000). A xenon flash, expected to produce a jump in the extracellular L-glutamate concentration, produced an inward current that rose to a steady level within 5 ms. The time course of the rise in current should be determined by the time course of the increase in extracellular L-glutamate concentration, the recording resolution of the patch-clamp system, and the transit time of glutamate through the transporter. The following observation indicates that the observed time course was determined primarily by the resolution of the recording system. A square pulse of current capacitatively injected at the input of the recording amplifier produced a response (part *B*) that had a time course similar to the response produced by photolysis of caged L-glutamate (part *A*, trace 2). The rise of either current in Fig. 16 can be approximately described by a single exponential with a time constant of 1·07 ms. The exponential curve is superimposed over the observed response in part *B*. The currents observed in eight cells could be fitted by an exponential with a time constant of $1{\cdot}3 \pm 0{\cdot}2$ ms (mean $\pm$ S.D.). The similarity in rise time of the responses in parts *A* and *B* indicates that a concentration jump produced an observed response whose onset was limited by the resolution of the recording system. Hence the transit time for L-glutamate influx must be faster than 1 ms.

Contribution to membrane polarization

The AAA-induced current can polarize a Müller cell. However, the total effect depends upon the other conductances expressed during physiological conditions. The experiment of Fig. 17*A* indicates that the normal contribution of the AAA transporter is small. The patch pipette contained a K^+-rich solution and the extracellular medium was a physiological saline. The voltage clamp was adjusted for zero holding current. During this condition the membrane potential is equal to the resting potential, in this case $-94{\cdot}8$ mV. A puff of 200 μM-D-aspartate from a nearby pipette produced a 195 pA response. Next, the voltage clamp was switched (at the first dotted line) to include a feed-back circuit that maintained zero injected current and allowed the voltage to change. In this 'normal voltage-recording' mode the voltage response produced by D-aspartate could be measured at the resting potential. Two puffs of D-aspartate each produced a 5·5 mV depolarization. Finally, voltage-clamp recording resumed (at the second dotted line) and a puff of D-aspartate was applied. In this experiment, activation of the AAA transporter produced a 195 pA inward current or a 5·5 mV depolarization. The small size of the depolarization is due

to a relatively low input resistance. For the cell illustrated in Fig. 17*A*, a 10 mV voltage-clamp step from the resting potential indicated a cell input resistance of 34 MΩ; in seven cells the range was 19–40 mΩ, values slightly larger than the 7·9 MΩ observed by Newman (1985*b*). A low input resistance maintained during physiological conditions allows activation of the AAA transporter to produce only a small voltage change. In contrast, Brew & Attwell (1987) claim that electrogenic AAA uptake is a 'major' current in salamander Müller cells and can significantly alter the membrane potential.

The resting membrane potential and input resistance of a Müller cell is normally determined by large K^+ currents (Newman 1985*a*, *b*; see also Kuffler, Nicholls & Orkand, 1966). The relative roles of K^+- and AAA-induced currents are illustrated for another cell in Fig. 17*B*. Membrane current was first recorded while the patch pipette was perfused with a solution containing 98 mM-K^+ and the cell was superfused with a solution containing 5 mM-K^+. Next, the cell was superfused with a solution containing 5 mM-Cs^+. The difference observed during the two conditions is an inwardly rectifying current that was blocked by replacing external K^+ with Cs^+ (trace 1). Subsequently, the patch pipette was perfused with a solution containing 98 mM-TEA^+. An outward K^+ current was blocked by replacing internal K^+ with TEA^+ (trace 2, see also Fig. 5*A*). Finally, the cell was exposed to 200 μM-D-aspartate. The AAA-induced current (trace 3) is smaller than either the inwardly or outwardly rectifying K^+ currents. The membrane potential and input resistance are primarily determined by the K^+ currents and the AAA-induced current can only make a small contribution.

DISCUSSION

Functional consequences

The concentration of AAA in the extracellular space depends upon the balance between influx and efflux. Because the intracellular volume within a tissue is 10× larger than the extracellular volume, the normal behaviour of the transporter is to mediate flux between a relatively large intracellular volume with a high amino acid concentration and a small extracellular volume with a much lower concentration. In this situation, the following argument demonstrates that voltage-dependent influx (Fig. 8) is sufficient to make the concentration of amino acid in the extracellular space a steep function of membrane voltage. Indeed, efflux may even be assumed to be constant and independent of voltage. A steady state for intracellular and extracellular concentrations is determined by intracellular metabolism, flux across the membrane, and diffusion from a transport site. If the rates for intracellular synthesis and for diffusion from a restricted extracellular space are slower than transport, then, on a short time scale, influx should balance efflux at each value of membrane potential. Our experiments demonstrate that influx is determined by two parameters: voltage, as specified in eqn (3), and extracellular concentration, as specified in eqn (1). Therefore, if the voltage is changed, the concentration in a small extracellular space can readjust until influx equals the constant efflux. The entire relation between extracellular concentration and voltage can be calculated if the concentration at one membrane potential, V^*, is known. Equation (1) can be written

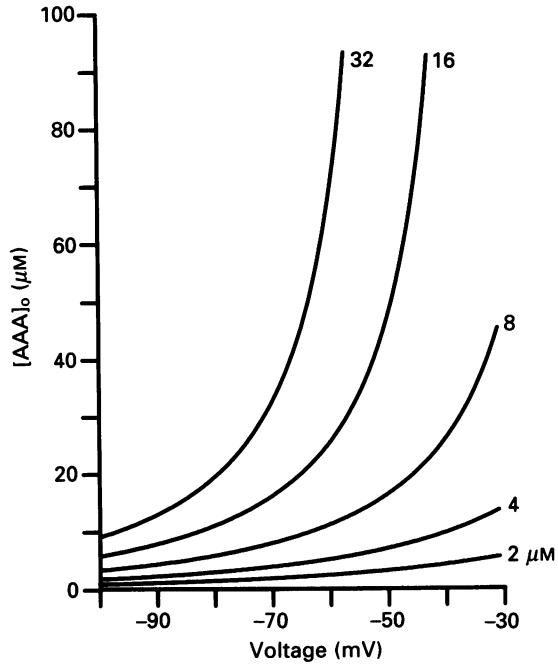

Fig. 18. Extracellular AAA concentration predicted from the observed behaviour of the AAA transporter. Each curve is the relation between voltage and extracellular concentration predicted if influx equals efflux (eqn (8)). Each curve assumes the same voltage-dependent influx but differs in the magnitude of the constant efflux. Influx depends on extracellular concentration (eqn (1)) and membrane voltage (eqn (3)). Efflux is constant and can be characterized by the extracellular concentration at a single voltage. The extracellular concentration at −70 mV is indicated to the right of each curve. The extracellular concentration becomes steeply dependent on voltage as the magnitude of the constant efflux increases.

for two values of membrane voltage, the fluxes set equal, and the resulting equation rearranged to yield

$$[\mathrm{Asp}]_o = K_{\mathrm{Asp}}[\mathrm{Asp}]_o^* I_{\max}^* / (K_{\mathrm{Asp}} I_{\max} + [\mathrm{Asp}]_o^* I_{\max} - [\mathrm{Asp}]_o^* I_{\max}^*), \quad (8)$$

where $I_{\max}$ and $I_{\max}^*$ are proportional to $Be^{-\beta V/\zeta}$. Each curve in Fig. 18 may be considered to be an 'isoflux' path, the relation between voltage and extracellular concentration predicted by constant unidirectional fluxes. Each curve assumes the same voltage-dependent influx but differs in the magnitude of the constant efflux. The dynamic balance between influx and efflux allows changes in membrane voltage to produce significant changes in extracellular AAA concentration. As the constant efflux is made larger, the concentration in the extracellular space becomes dramatically voltage dependent. This result was derived with the assumption that efflux is voltage independent. If, however, depolarization increases efflux, then the voltage dependence for extracellular concentration would be an even steeper function of voltage.

During physiological conditions, large K^+ conductances (Fig. 17) keep glial cells

hyperpolarized. Moreover, a low input resistance makes the membrane potential relatively insensitive to the current produced by changes in extracellular AAA concentration. Consequently, glial cells are normally optimized for a constant and maximal glutamate influx. However, during pathological conditions, extracellular K^+ may accumulate, glia may depolarize, and influx may slow. The result would be an increase in extracellular glutamate concentration (see Fig. 18) which can depolarize neurons and induce an additional release of K^+ and glutamate. A regenerative cycle of neuron depolarization, extracellular K^+ accumulation, glial depolarization and extracellular glutamate accumulation may produce a wave of spreading depression.

Select neurons also have amino acid transporters. Because they have a significant difference in their intracellular metabolism and change their membrane voltage, the transporter we have observed in the Müller cell would behave differently if expressed in a neuron. Glia, with abundant glutamine synthetase (Ghandour, Langley, Vincendon & Gombos, 1979; Roots, 1982), readily convert glutamate to glutamine and may maintain a lower internal concentration of glutamate than do neurons. Consequently, the efflux of glutamate could be greater from neurons than from glia. In this case, Fig. 18 predicts that the concentration of amino acids in the extracellular space would have a steeper voltage dependence within the physiological range.

Unlike glia, neurons can change their membrane voltage and may modulate the balance between influx and efflux. Transporters appear to release AAA from photoreceptors (Miller & Schwartz, 1983), to release GABA from horizontal cells (Schwartz, 1982, 1987; Ayoub & Lam, 1984), and to mediate synaptic transmission during conditions unfavourable for exocytosis (Schwartz, 1986). The efflux of GABA from an isolated horizontal cell has been detected by the appearance of a GABA-sensitive current in an apposed bipolar cell (Schwartz, 1987). Pushing a horizontal and bipolar cell together could trap an extracellular space between them. The GABA concentration in this space should be in a dynamic balance controlled by efflux and influx. Indeed, the voltage-dependent communication observed between solitary horizontal and bipolar cells (Fig. 4*B* in Schwartz, 1987) is remarkably similar to the prediction of an isoflux line in Fig. 18.

Mechanism of transport

Charged molecules, unable to penetrate a lipid bilayer, cross biological membranes with the help of pores and carriers. During recent years, the electrical behaviour of pores has been intensively studied. Less attention has been devoted to carriers. Usually pores and carriers are assumed to operate by different mechanisms. An open pore allows ions to enter from either end and pass through to the opposite side. The behaviour of carriers is believed to be more complex. Their specificity for selected substrates indicates that carriers have binding sites that discriminate between close chemical analogues. Although direct observations are lacking, these binding sites are usually assumed to be accessible at a single instant from only one side of the membrane. As a consequence, carriers have been assumed to operate with a mobile or transitional element that alternates between two conformations and exposes binding sites to substrates entering first from one side of a membrane and then from

the other (see for example Walmsley, 1988). The conformational shift might move binding sites across the membrane or simultaneously close entry into the carrier from one surface and open egress towards the opposite surface.

One type of model assumes that a binding site is moved across the membrane. The availability at each membrane surface of a charged binding site would be influenced by membrane voltage. Since AAA influx is electrogenic, the occupied and unoccupied binding sites would have different net charge. Consequently, the distribution of the bound and unbound site would be differentially affected by voltage. If the binding site is mobile, then its distribution within the membrane will depend upon both the external AAA concentration and membrane voltage. The glutamate transporter does not display this type of behaviour. The shape of the current–voltage relation does not depend upon the extracellular AAA concentration (Fig. 9). Consequently, transport is not produced by the movement of a mobile binding site across the membrane.

Another type of carrier model would keep a binding site at a fixed position but allow a cycle of conformational change to provide access from first one solution and then the opposite solution. The current–voltage relation need not be affected by AAA concentration. But the functional asymmetry that results in electrogenic influx (Fig. 8) and electroneutral efflux (Fig. 10) as well as the coupling between influx and efflux (Fig. 11) are not easily explained with only one binding site.

The transporter behaves, in some respects, more like a pore frozen in its open state than a carrier that undergoes a conformational change. Transport can be explained by the diagrams in Fig. 19 which portray Na^+ and an AAA moving between binding sites with fixed positions. However, while pores allow single ions to pass, the transporter allows a complex of an amino acid and Na^+ to pass. Access to the transporter is determined by binding sites that are outside the membrane field. External Na^+ enters its binding sites in the absence of an AAA (diagram 1) and can leak through the transporter (diagram 2). External AAA does not interact with the transporter in the absence of Na^+. The binding of three Na^+ ions and one AAA at the external surface (diagram 3) enables AAA influx (diagram 4). The movement of two Na^+ ions with each AAA (equal to a $+1$ net charge) would produce an inward current. The movement of all three Na^+ ions with each AAA (equal to a $+2$ net charge) is unlikely if Coulombic repulsion between positive charges destabilizes the co-ordinate movement of a polyvalent complex through a membrane pore. Our experiments do not indicate the number of Na^+ ions that bind at the internal surface, but only one Na^+ ion appears to move outward with each AAA molecule (diagram 6). No other ion appears to co-migrate.

Coupling between influx and efflux can also be explained by the model illustrated in Fig. 19. *Trans*-inhibition (Fig. 10) is readily explained if an AAA penetrates the pore and then occupies a previously empty site. Flux would be impeded when an AAA that moves through the transporter encounters a *trans* site that is already occupied. An explanation for *trans*-stimulation is more complex. *Trans*-stimulation by external AAA is voltage dependent and appears to be proportional to the influx of Na^+ and AAA (Fig. 11). The mechanism of *trans*-stimulation may depend upon the inward movement of Na^+. For example, an AAA and Na^+ might penetrate the pore (diagram 4) and leave a Na^+ occupying an internal site (diagram 5). The Na^+ that remains could facilitate the binding of a new amino acid molecule which might then

efflux (diagram 6). Na^+ binding sites would be filled either when Na^+ moves through the transporter or when Na^+ enters from the adjacent solution. *Trans*-stimulation would occur when Na_2-AAA influx significantly increases the probability that the internal Na^+ site is filled.

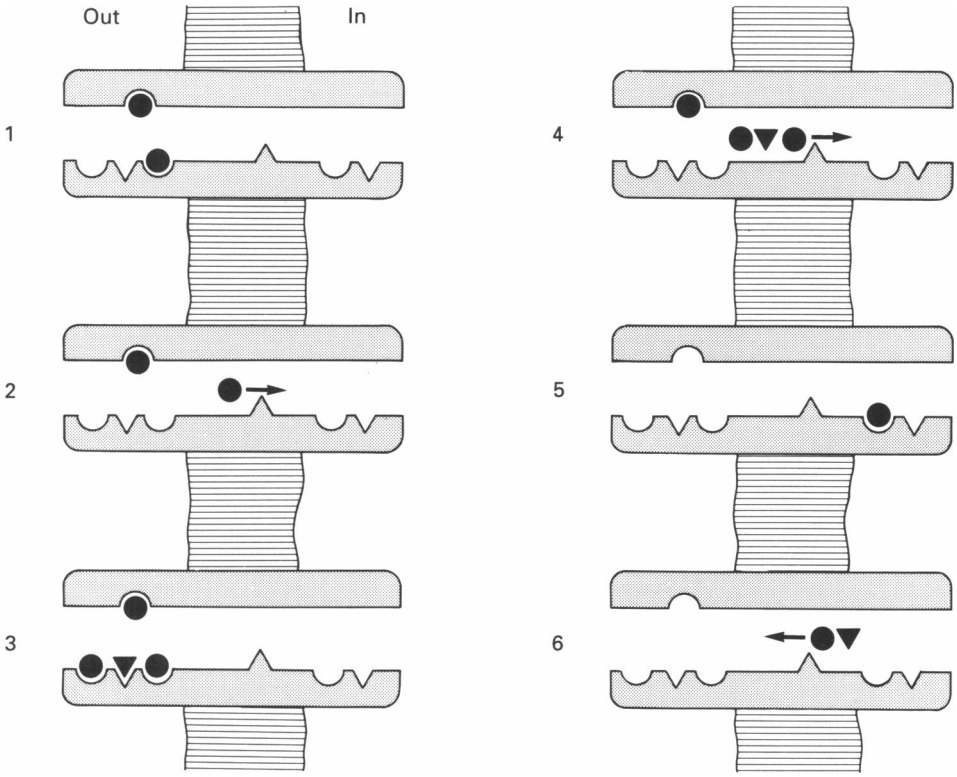

Fig. 19. A model for AAA transport. The six states referred to in the text are pictured and numbered. Binding sites are outside the membrane field. A single energy barrier is positioned within a *trans*-membrane pore. The transporter can be permeated by ions or complexes with either zero net charge (Na-AAA) or +1 net charge (Na^+ or $[Na_2\text{-AAA}]^+$). Na^+ can bind in the absence of AAA at external sites (diagram 1) and move through the transporter (diagram 2). The binding of an AAA and three Na^+ ions is required for AAA-induced electrogenic influx (diagram 3). However, only an AAA and two Na^+ ions need translocate to produce a current (diagram 4). The internal surface may have only a binding site for one Na^+ ion and a site for an AAA (diagram 5). Efflux (diagram 6) would be electroneutral. Asymmetry in function is produced by an asymmetry in the number and affinities of fixed binding sites at the two surfaces. ●, Na^+; ▼, AAA.

The estimated times for translocation through the AAA transporter and small pores are not very different. Each transporter molecule is estimated to produce a current (at 20 °C and −70 mV) of 1·6 fA, equivalent to each positive charge passing through the transporter in 100 μs (see Figs 15 and 16, and associated text). By comparison, the cyclic GMP-regulated pore in vertebrate photoreceptors conducts a current of 2–4 fA (see Yau & Baylor, 1989), equivalent to a transit time of 40–80 μs. Carriers may be more like pores than heretofore suspected. The model in Fig. 19 was designed to blur the difference.

We are indebted to Dr J. A. Wasserstrom and Ms Marie Norell for fabricating Na^+ electrodes. Supported by National Institutes of Health research grant EY-02440; a grant from the Brain Research Foundation, the University of Chicago; from the Naito Foundation; and by Grants in Aid for Scientific Research from the Ministry of Education, Science and Culture, Japan.

REFERENCES

AYOUB, G. S. & LAM, D. M. K. (1984). The release of γ-aminobutryic acid from horizontal cells of the goldfish (*Carassius auratus*) retina. *Journal of Physiology* **355**, 191–214.

BADER, C. R., MACLEISH, P. R. & SCHWARTZ, E. A. (1979). A voltage-clamp study of the light response in solitary rods of the tiger salamander. *Journal of Physiology* **296**, 1–26.

BARBOUR, B., BREW, H. & ATTWELL, D. (1988). Electrogenic glutamate uptake in glial cells is activated by intracellular potassium. *Nature* **335**, 433–435.

BENNETT, J. P., MULDER, A. H. & SNYDER, S. H. (1974). Neurochemical correlates of synaptically active amino acids. *Life Sciences* **15**, 1045–1056.

BREW, H. & ATTWELL, D. (1987). Electrogenic glutamate uptake is a major current in the membrane of axolotl retinal glial cells. *Nature* **327**, 707–709.

CHANDLER, W. K. & MEVES, H. (1965). Voltage clamp experiments on internally perfused giant axons. *Journal of Physiology* **180**, 788–820.

CHOI, D. W. (1988). Glutamate neurotoxicity and diseases of the nervous system. *Neuron* **1**, 623–634.

DEVRIES, S. H. & SCHWARTZ, E. A. (1989). Modulation of an electrical synapse between solitary pairs of catfish horizontal cells by dopamine and second messengers. *Journal of Physiology* **414**, 351–375.

ERECINSKA, M. (1987). The neurotransmitter amino acid transport systems. *Biochemical Pharmacology* **36**, 3547–3555.

ERECINSKA, M., WANTORSKY, D. & WILSON, D. F. (1983). Aspartate transport in synaptosomes from rat brain. *Journal of Biological Chemistry* **258**, 9069–9077.

FAGG, G. E. & LANE, J. D. (1979). The uptake and release of putative amino acid neurotransmitters. *Neuroscience* **4**, 1015–1036.

FIDLER, N., ELLIS-DAVIES, G., KAPLAN, J. H. & MCCRAY, J. A. (1988). Rate of Ca^{2+} release following laser photolysis of a new caged Ca^{2+}. *Biophysical Journal* **53**, 599a.

FOSTER, A. C. & FAGG, G. E. (1984). Acidic amino acid binding sites in mammalian neuronal membranes: their characteristics and relationship to synaptic receptors. *Brain Research Reviews* **7**, 103–164.

FRANKENHAEUSER, B. & MOORE, L. E. (1963). The effect of temperature on the sodium and potassium permeability changes in myelinated nerve fibres of *Xenopus laevis*. *Journal of Physiology* **169**, 431–437.

GAGE, P. W. & VAN HELDEN, D. (1979). Effects of permeant monovalent cations on end-plate channels. *Journal of Physiology* **288**, 509–528.

GAZZOLA, G. C., DALL'ASTA, V., BUSSOLATI, O., MAKOWSKE, M. & CHRISTENSEN, H. N. (1981). A stereoselective anomaly in dicarboxylic amino acid transport. *Journal of Biological Chemistry* **256**, 6064–6059.

GHANDOUR, M. S., LANGLEY, O. K., VINCENDON, G. & GOMBOS, G. (1979). Double labeling immunohistochemical technique provides evidence of the specificity of glial markers. *Journal of Histochemistry and Cytochemistry* **27**, 1634–1637.

HAMILL, O. P., MARTY, A., NEHER, E., SAKMANN, B. & SIGWORTH, F. J. (1981). Improved patch-clamp techniques for high-resolution current recording from cells and cell-free membrane patches. *Pflügers Archiv* **391**, 85–100.

HILLE, B. (1972). The permeability of the sodium channel to metal cations in myelinated nerve. *Journal of General Physiology* **59**, 637–658.

KANNER, B. I. & SHARON, I. (1978). Solubilization and reconstitution of the L-glutamic acid transporter from rat brain. *FEBS Letters* **94**, 245–248.

KORENBROT, J. I., PERRY, R. & COPENHAGEN, D. R. (1987). Development and characterization of a polymer gel with an immobilized enzyme to measure L-glutamate. *Analytical Biochemistry* **161**, 187–199.

KUFFLER, S. W., NICHOLLS, J. G. & ORKAND, R. K. (1966). Physiological properties of glial cells in the central nervous system of amphibia. *Journal of Neurophysiology* **29**, 768–787.

KUFFLER, S. W. & YOSHIKAMI, D. (1975). The number of transmitter molecules in a quantum: an estimate from iontophoretic application of acetylcholine at the neuromuscular synapse. *Journal of Physiology* **251**, 465–482.

LESTER, H. A. & NERBONNE, J. M. (1982). Physiological and pharmacological manipulations with light flashes. *Annual Review of Biophysics and Bioengineering* **11**, 151–175.

MAYER, M. L., WESTBROOK, G. L. & GUTHRIE, P. B. (1984). Voltage-dependent block by Mg^{2+} of NMDA responses in spinal cord neurones. *Nature* **309**, 261–263.

MILLER, A. M. & SCHWARTZ, E. A. (1983). Evidence for the identification of synaptic transmitters released by photoreceptors of the toad retina. *Journal of Physiology* **334**, 325–349.

MOORE, J. W. & PEARSON, R. G. (1981). *Kinetics and Mechanism*. John Wiley, New York.

NELSON, M. T. & BLAUSTEIN, M. P. (1982). GABA efflux from synaptosomes: Effects of membrane potential, and external GABA and cations. *Journal of Membrane Biology* **69**, 213–223.

NEWMAN, E. A. (1985*a*). Voltage-dependent calcium and potassium channels in retinal glial cells. *Nature* **317**, 809–811.

NEWMAN, E. A. (1985*b*). Membrane physiology of retinal glial (Müller) cells. *Journal of Neuroscience* **5**, 2225–2239.

NICHOLLS, D. G., SIHRA, T. S. & SANCHEZ-PRIETO, S. (1987). Calcium-dependent and -independent release of glutamate from synaptosomes monitored by continuous fluorometry. *Journal of Neurochemistry* **49**, 50–57.

NOWAK, L., BREGESTOVSKI, P., ASCHER, P., HERBERT, A. & PROCHIANTZ, A. (1984). Magnesium gates glutamate-activated channels in mouse central neurones. *Nature* **307**, 462–465.

OLNEY, J. W., HO, O. L. & RHEE, V. (1971). Cytotoxic effects of acidic and sulphur containing amino acids on the infant mouse central nervous system. *Experimental Brain Research* **14**, 61–76.

ORBACH, E. & FINKELSTEIN, A. (1980). The nonelectrolyte permeability of planar lipid bilayer membranes. *Journal of General Physiology* **75**, 427–436.

PETERSON, N. A. & RAGHUPATHY, E. (1974). Selective effects of lithium on synaptosomal amino acid transport systems. *Biochemical Pharmacology* **23**, 2491–2494.

RINK, T. J., TSIEN, R. Y. & POZZAN, T. (1982). Cytoplasmic pH and free Mg^{2+} in lymphocytes. *Journal of Cell Biology* **95**, 189–196.

ROOTS, B. I. (1982). Comparative studies on glial markers. *Journal of Experimental Biology* **95**, 167–180.

SCHWARTZ, E. A. (1982). Calcium-independent release of GABA from isolated horizontal cells of the toad retina. *Journal of Physiology* **323**, 211–227.

SCHWARTZ, E. A. (1986). Synaptic transmission in amphibian retinae during conditions unfavourable for calcium entry into presynaptic terminals. *Journal of Physiology* **376**, 411–428.

SCHWARTZ, E. A. (1987). Depolarization without calcium can release γ-aminobutyric acid from a retinal neuron. *Science* **238**, 350–355.

SOEJIMA, M. & NOMA, A. (1984). Mode of regulation of the ACh-sensitive K-channel by the muscarinic receptor in rabbit atrial cells. *Pflügers Archiv* **400**, 424–431.

STEINER, R. A., OEHME, M., AMMANN, D. & SIMON, W. (1979). Neutral carrier sodium ion-selective microelectrode for intracellular studies. *Analytical Chemistry* **51**, 351–353.

USOWICZ, M. M., GALLO, V. & CULL-CANDY, S. G. (1989). Multiple conductance channels in type-2 cerebellar astrocytes activated by excitatory amino acids. *Nature* **339**, 380–383.

WATKINS, J. C. & OLVERMAN, H. J. (1987). Agonists and antagonists for excitatory amino acid receptors. *Trends in Neurosciences* **10**, 265–272.

WEAST, R. C. & ASTLE, M. J. (1981). *CRC Handbook of Chemistry and Physics*. CRC Press, Boca Raton, FL.

WALMSLEY, A. R. (1988). The dynamics of the glucose transporter. *Trends in Biochemical Sciences* **13**, 226–231.

YAU, K.-W. & BAYLOR, D. A. (1989). Cyclic GMP-activated conductance of retinal photoreceptor cells. *Annual Review of Neuroscience* **12**, 289–327.